

## New form of dispersion tensor for axisymmetric porous media with implementation in particle tracking

Peter C. Lichtner, Sharad Kelkar, and Bruce Robinson

Los Alamos National Laboratory, Los Alamos, New Mexico, USA

Received 16 November 2000; revised 24 January 2002; accepted 4 March 2002; published 17 August 2002.

[1] A general form of the dispersion tensor is derived for axisymmetric porous media involving four dispersivity coefficients corresponding to longitudinal and transverse dispersion in horizontal and vertical directions, defined as perpendicular and parallel to the axis of symmetry, respectively. The general form of the dispersion tensor provides for distinct vertical and horizontal longitudinal dispersivity values. Transverse dispersion is isotropic for flow parallel to the symmetry axis and anisotropic for flow perpendicular to the symmetry axis with distinct horizontal and vertical transverse dispersivities. The new form of the dispersion tensor is applied to several examples involving axisymmetric media utilizing particle tracking techniques and compared to the tensor proposed by *Burnett and Frind* [1987]. It is demonstrated that for the case of spatially variable flow the drift term  $\nabla \cdot (\phi \mathbf{D})/\phi$  must generally be included in the particle tracking algorithm to obtain accurate results. *INDEX TERMS:* 1829 Hydrology: Groundwater hydrology; 1832 Hydrology: Groundwater transport; 2199 Interplanetary Physics: General or miscellaneous; *KEYWORDS:* anisotropy, dispersion, particle tracking, transport

### 1. Introduction

[2] Several attempts have been made in the past to describe dispersion in axisymmetric porous media [*Burnett and Frind*, 1987; *Jensen et al.*, 1993]. *Zheng and Bennett* [1995] used the form of the dispersion tensor proposed by *Burnett and Frind* [1987] for describing transport of a tracer in axisymmetric media. The term axisymmetric refers to layered media that possess an axis of symmetry, rotations about which leave the system unaltered. A characteristic feature of axisymmetric media is the nonisotropic nature of transverse dispersion for flow perpendicular to the axis of symmetry. In addition, it would be expected that longitudinal dispersion should in general be different for flow parallel or perpendicular to the symmetry axis. In the above mentioned papers, flow was restricted to be approximately perpendicular to the symmetry axis. Furthermore, the forms of the dispersion tensor that were used were based on heuristic considerations. *Jensen et al.* [1993] appear to be the only authors who attempted to introduce separate longitudinal dispersivities for horizontal and vertical flow parallel and perpendicular to the axis of symmetry. However, because these authors only considered diagonal terms, a physical interpretation of the dispersivity coefficients is difficult to make.

[3] The main purpose of this contribution is to develop a new form of the dispersion tensor applicable to axisymmetric media with flow at an arbitrary angle to the symmetry axis. For this purpose the form of the dispersion tensor developed by *Poreh* [1965] based on the work of *Robertson* [1940] on invariants in isotropic turbulence theory is used. Symmetry arguments are used to restrict the form of the dispersion tensor applicable to porous media with a rotational axis of symmetry. For a general anisotropic medium

the dispersion tensor is more complex, involving possibly as many as 21 to 36 independent parameters, depending on the symmetries invoked [*Scheidegger*, 1961; *Bear*, 1972]. The approach developed by *Poreh* [1965] allows for four independent parameters. The principal axis of the dispersion tensor need not be necessarily aligned with the direction of flow [*Poreh*, 1965]. For flow parallel and perpendicular to the symmetry axis, the new form of the dispersion tensor reduces to the special forms appropriate for these cases. Thus for flow parallel to the symmetry axis, transverse dispersion is isotropic, whereas for flow perpendicular to the symmetry axis it becomes anisotropic. It should be noted that issues related to the scale dependence of dispersion are not considered. Rather, a conventional Fickian representation of dispersion is assumed which may be taken as the asymptotic limiting form of the dispersion tensor [*Neuman*, 1990].

[4] A comment is in order for pursuing modification to the multi-Gaussian formulation of dispersion which results in the classical Fickian form used here. While this approach is known to have several serious limitations, such as backward dispersion against the direction of flow and scale independence, nevertheless it is still widely used in a number of practical applications. Furthermore, it may be the only approach for representing local scale dispersion. For these reasons we feel it is still useful to generalize the Fickian approach to axisymmetric media.

[5] The new form of the dispersion tensor is implemented in particle tracking methods and applied to axisymmetric nonisotropic media. The particle tracking approach has been widely applied to model dispersive transport in homogeneous and heterogeneous isotropic media for both reactive [*Ahlstrom et al.*, 1977; *Fabriol et al.*, 1993] and nonreactive transport [*Kinzelbach and Uffink*, 1991; *Tchelepi et al.*, 1993; *Tompson*, 1993; *Tompson and Dougherty*, 1988; *Tompson and Gelhar*, 1990; *Tompson et al.*, 1996; *LaBolle et al.*, 1996]. Particle tracking methods offer an attractive

alternative to finite difference techniques for solving solute transport equations in both homogeneous and heterogeneous media. In this approach, continuum transport equations are replaced by a discrete set of particles that are transported by advection subject to Brownian motion to represent diffusion and dispersion. Given a sufficient numbers of particles, continuum and particle tracking models are equivalent.

[6] Conventional finite difference approaches, when applied to large-scale problems, suffer from numerical dispersion caused by the need to use large grid blocks to limit the number of nodes to reasonable values. To obtain a stable solution, upstream weighting is often invoked which dramatically smears out sharp fronts. Furthermore, the computation time involved in particle tracking is proportional to the number of particles used in the simulation, whereas finite difference methods are proportional to the number of nodes which may number on the order of  $10^6$  or more. Particle tracking also involves more moderate storage requirements compared to finite difference methods.

[7] A primary advantage particle-tracking methods have over conventional finite difference approaches is the apparent ease with which the full dispersion tensor can be incorporated into the transport equations. However, it must be noted in this regard that proper treatment of discontinuous media using particle tracking is still an area of active research and the effects of interpolation error along particle paths needs further investigation [see, e.g., *LaBolle et al.*, 1996]. Finite difference methods require incorporation of the off-diagonal terms of the dispersion tensor when modeling transport in heterogeneous media with variable fluid velocity, or in cases where the fluid velocity is not aligned with one of the coordinate axes. This requires enlarging the finite difference stencil from 5 to 9 points in 2D, and from 7 to 27 points in 3D. Besides increasing the bandwidth of the Jacobian matrix in the linear solver, stability issues arise in terms of its positive definiteness. This can lead to oscillatory behavior which is unacceptable for reactive transport simulation [*Cirpka et al.*, 1999]. Particle tracking methods by contrast provide an efficient numerical algorithm without these deficiencies for modeling large-scale transport of tracers in heterogeneous porous media.

## 2. Dispersion Tensor for Axisymmetric Media

### 2.1. Eulerian Mass Conservation Equation

[8] The equation of motion describing the evolution of a plume in a saturated porous medium corresponding to a nonreactive, dilute solute species with concentration  $C$ , is given by the mass conservation equation

$$\frac{\partial}{\partial t}(\phi C) + \nabla \cdot (\mathbf{q}C - \phi \mathbf{D} \nabla C) = 0, \quad (1)$$

referred to as the advection-diffusion-dispersion equation. In this equation  $t$  refers to time, and  $\nabla = (\partial/\partial x, \partial/\partial y, \partial/\partial z)$ . The coefficients  $\phi$ ,  $\mathbf{q}$ , and  $\mathbf{D}$ , appearing in the advection-diffusion-dispersion equation refer to the porosity of the porous medium, the Darcy velocity, and the diffusion/disposition tensor, respectively. Generally these quantities vary spatially and temporally. Experimental studies of transport in groundwater have been compiled to determine the nature of the dispersion tensor and the numerical values

of the dispersivity. *Gelhar* [1997] showed that distinct values of the longitudinal dispersivity, the transverse dispersivity in the horizontal direction, and the transverse dispersivity in the vertical direction can be identified based on available field transport studies. The general conceptual model underlying the use of these three terms is one of horizontal flow with tortuous fine-scale flow through heterogeneous media. The details of transport through the heterogeneous media give rise to spreading of solute in the direction of flow and, to a lesser extent, transverse to the direction of flow. Of course, groundwater flow, though generally horizontal, exhibits vertical velocities locally in regions of upward or downward gradients, such as in areas of recharge or discharge or when the flow is subject to variability in hydraulic conductivity that diverts water vertically.

[9] In practice, it is difficult, from available data, to propose more complex forms of the dispersion process and to determine the alternate dispersivity values from field observations. Nevertheless, it is quite possible that more complex forms are more representative, given the complexity and variety of different heterogeneities present in nature. An important conclusion from the available field data is that longitudinal dispersion is a strong function of scale, that is, the travel length of a solute plume in the medium [e.g., *Neuman*, 1990]. In a typical groundwater flow model at the scale of a flow basin, characteristic flow distances of tens to hundreds of meters vertically may be present, compared to hundreds to thousands of meters horizontally. Given the difference in scale, it is not clear that the longitudinal dispersivity in the vertical direction should be set equal to that in the horizontal direction. In addition, in stratified porous media containing heterogeneities such as irregular shaped beds or clay lenses, the characteristic scale of the heterogeneity encountered by a solute will be different in the horizontal and vertical directions, yielding potentially different longitudinal dispersion. Therefore one motivation of the development of the theory in this section is to propose a dispersion tensor that can be used to handle these more general scenarios.

### 2.2. General Form of the Dispersion Tensor for Axisymmetric Media

[10] Consider a porous medium that, at the macroscale, exhibits an axis of symmetry  $\lambda$ . As a consequence, physical processes are invariant under rotations about the axis of symmetry. To be considered a tensor, the collection of coefficients making up the dispersion tensor must satisfy certain transformation rules upon changing from one coordinate system to another. The form of the dispersion tensor is obtained by assuming the scalar invariant

$$\mathcal{D}(\mathbf{a}, \mathbf{b}) = \sum_{ij} D_{ij} a_i b_j, \quad (2)$$

defined as the contraction of the dispersion tensor with arbitrary vectors  $\mathbf{a}$  and  $\mathbf{b}$ , can be expressed in terms of the fundamental invariants  $\mathbf{a} \cdot \mathbf{b}$ ,  $\mathbf{a} \cdot \mathbf{v}$ ,  $\mathbf{a} \cdot \lambda$ , . . . , constructed from the vectors  $\mathbf{a}$ ,  $\mathbf{b}$ ,  $\mathbf{v}$ , and  $\lambda$  where  $\mathbf{v} = \mathbf{q}/\phi$  denotes the average macroscale pore velocity. Invariants formed from vector products, for example  $\mathbf{a} \times \mathbf{b} \cdot \mathbf{v}$ , are not allowed because they change sign on reflection of the coordinate system. The theory to construct such an object was

presented in the turbulence literature by *Robertson* [1940] and later applied to dispersion by *Poreh* [1965]. It can be shown that the most general, symmetric, second order tensor that can be constructed from these the vectors  $\mathbf{v}$  and  $\boldsymbol{\lambda}$  is given by the dyadic [*Poreh*, 1965; *Batchelor*, 1959]

$$\mathbf{D} = \alpha_1 v \mathbf{I} + \alpha_2 \frac{\mathbf{v}\mathbf{v}}{v} + \alpha_3 v \boldsymbol{\lambda} \boldsymbol{\lambda} + \frac{1}{2} \alpha_4 (\boldsymbol{\lambda}\mathbf{v} + \mathbf{v}\boldsymbol{\lambda}), \quad (3)$$

where  $\mathbf{I}$  represents the unit dyadic,  $v$  denotes the magnitude of the solute velocity ( $v^2 = \sum v_i^2$ ), and the coefficients  $\alpha_i$  are scalar quantities with the dimension of length. Symmetry is imposed on the dispersion tensor. While traditionally this assumption is made for the dispersion tensor [*Bear*, 1972], it is not a fundamental requirement. In this expression for the dispersion tensor, and in what follows, the contribution of molecular diffusion is not explicitly indicated for simplicity. It may be easily added to the diagonal elements. For a general discussion of the properties of dyadics consult, e.g., *Morse and Feshback* [1953].

[11] The four coefficients  $\alpha_i$  that appear in equation (3) are in general functions of the scalar quantities  $v$  and  $\boldsymbol{\lambda} \cdot \mathbf{v}$ , which may be functions of time and space for a variable velocity field, for example, such as encountered in heterogeneous media for example. If  $\mathbf{v}$  is an eigenvector of  $\mathbf{D}$ , the coefficients  $\alpha_i$  may be related to their more conventional designations in terms of longitudinal and transverse dispersivity corresponding to eigenvalues of  $\mathbf{D}$  associated with principal axes parallel and perpendicular to the direction of flow, respectively. In this case, two distinct longitudinal and transverse dispersivities can be defined. These correspond to flow parallel and perpendicular to the axis of symmetry, and may be assigned as  $\alpha_L^H$ ,  $\alpha_L^V$  and  $\alpha_T^H$ ,  $\alpha_T^V$ , respectively. The superscripts  $V$  and  $H$ , designating “vertical” and “horizontal”, are defined in relation to the axis of symmetry with  $V$  parallel and  $H$  perpendicular to the symmetry axis  $\boldsymbol{\lambda}$ . For a general axisymmetric medium, however, it is possible that the principal axes are not aligned with the direction of flow, and in that case the terms longitudinal and transverse are not meaningful.

[12] As will turn out in the analysis given below, the flow velocity  $\mathbf{v}$  is an eigenvector of the dispersion tensor provided that the coefficients  $\alpha_3$  and  $\alpha_4$  are appropriately related to one another [see equation (17)]. As a result, for this case there are three independent coefficients and an equal number of eigenvalues. For the more general case where  $\mathbf{v}$  is not an eigenvector, all four coefficients  $\alpha_i$  are independent.

### 2.3. Eigenvalues and Eigenvectors of the Dispersion Tensor $\mathbf{D}$

[13] The eigenvalues and eigenvectors of  $\mathbf{D}$  provide an interpretation of the coefficients  $\alpha_i$  in terms of the more physically meaningful longitudinal and transverse dispersivity coefficients. The eigenvalue problem for  $\mathbf{D}$  with eigenvalues  $\mu_i v$  and eigenvectors  $\boldsymbol{\zeta}_i$  is defined as

$$\mathbf{D} \cdot \boldsymbol{\zeta}_i = \mu_i v \boldsymbol{\zeta}_i, \quad (i = 1, 2, 3). \quad (4)$$

First note that the vector  $\boldsymbol{\zeta}_3 = \mathbf{v} \times \boldsymbol{\lambda}$ , perpendicular to the plane defined by the vectors  $\mathbf{v}$  and  $\boldsymbol{\lambda}$ , is always an eigenvector of  $\mathbf{D}$  belonging to the eigenvalue  $\alpha_1 v$  since

$$\mathbf{D} \cdot \boldsymbol{\zeta}_3 = \alpha_i v \boldsymbol{\zeta}_3, = \alpha_T^H \boldsymbol{\zeta}_3, \quad (5)$$

in which in the latter expression  $\alpha_1$  is identified with  $\alpha_T^H$ , the horizontal transverse dispersivity coefficient. As a consequence, the remaining two eigenvectors of  $\mathbf{D}$ , denoted by  $\boldsymbol{\zeta}_1$  and  $\boldsymbol{\zeta}_2$ , must lie in the plane defined by  $\mathbf{v}$  and  $\boldsymbol{\lambda}$ . Without additional restrictions on the coefficients  $\alpha_i$ , neither eigenvector need coincide with the fluid velocity  $\mathbf{v}$  [*Poreh*, 1965].

[14] To determine the remaining two eigenvalues and corresponding eigenvectors of  $\mathbf{D}$ , the eigenvectors are expanded in terms of an orthogonal set of vectors which lie in the plane perpendicular to  $\boldsymbol{\zeta}_3$ . It is useful to introduce the vector  $\boldsymbol{\omega}$  constructed orthogonal to  $\mathbf{v}$  using the Gram-Schmidt orthogonalization procedure to give

$$\boldsymbol{\omega} = \boldsymbol{\lambda} - \frac{\boldsymbol{\lambda} \cdot \mathbf{v}}{v^2} \mathbf{v} = \boldsymbol{\lambda} - \frac{\cos \theta}{v} \mathbf{v}, \quad (6)$$

where

$$\cos \theta = \frac{\boldsymbol{\lambda} \cdot \mathbf{v}}{v}, \quad (7)$$

with  $\theta$  the angle between  $\boldsymbol{\lambda}$  and  $\mathbf{v}$ . It follows that

$$\boldsymbol{\omega} \cdot \mathbf{v} = 0, \quad \text{and} \quad \boldsymbol{\omega}^2 = \boldsymbol{\omega} \cdot \boldsymbol{\omega} = 1 - \cos^2 \theta. \quad (8)$$

Using the orthogonal vectors  $\mathbf{v}$  and  $\boldsymbol{\omega}$ , one can write the expansion for normalized eigenvectors

$$\boldsymbol{\zeta}_i = \frac{\gamma_i \mathbf{v} + \beta_i \boldsymbol{\omega}}{\sqrt{\gamma_i^2 v^2 + \beta_i^2 \boldsymbol{\omega}^2}}, \quad (9)$$

with expansion coefficients  $\gamma_i$  and  $\beta_i$ . Expressing  $\mathbf{D}$  in terms of  $\mathbf{v}$  and  $\boldsymbol{\omega}$  yields

$$\begin{aligned} \mathbf{D} = \alpha_1 v \mathbf{I} &+ [\alpha_2 + \cos^2 \theta \alpha_3 + \cos \theta \alpha_4] \frac{\mathbf{v}\mathbf{v}}{v} + \alpha_3 v \boldsymbol{\omega} \boldsymbol{\omega} \\ &+ \left( \cos \theta \alpha_3 + \frac{1}{2} \alpha_4 \right) (\boldsymbol{\omega}\mathbf{v} + \mathbf{v}\boldsymbol{\omega}). \end{aligned} \quad (10)$$

Expanding  $\mathbf{D} \cdot \mathbf{v}$  and  $\mathbf{D} \cdot \boldsymbol{\omega}$  in terms of the vectors  $\mathbf{v}$  and  $\boldsymbol{\omega}$  gives

$$\mathbf{D} \cdot \mathbf{v} = a \mathbf{v} + b \boldsymbol{\omega}, \quad (11a)$$

and

$$\mathbf{D} \cdot \boldsymbol{\omega} = c \mathbf{v} + d \boldsymbol{\omega}. \quad (11b)$$

The expansion coefficients  $a$ ,  $b$ ,  $c$ , and  $d$  are defined as

$$a = (\alpha_1 + \alpha_2 + \cos^2 \theta \alpha_3 + \cos \theta \alpha_4) v, \quad (12a)$$

$$b = \left( \cos \theta \alpha_3 + \frac{1}{2} \alpha_4 \right) v^2, \quad (12b)$$

$$c = (1 - \cos^2 \theta) \left[ \cos \theta \alpha_3 + \frac{1}{2} \alpha_4 \right], \quad (12c)$$

and

$$d = [\alpha_1 + (1 - \cos^2 \theta) \alpha_3] v. \quad (12d)$$

From these results the matrix equation for the eigenvalues and eigenvectors follows

$$\begin{bmatrix} (a - \mu_i) + c \\ a + (d - \mu_i) \end{bmatrix} \begin{bmatrix} \gamma_i \\ \beta_i \end{bmatrix} = 0. \quad (13)$$

The secular equation has as solution the eigenvalues

$$\mu_i = \frac{1}{2v} \left[ a + d \pm \sqrt{(a - d)^2 + 4bc} \right]. \quad (14)$$

The plus sign corresponds to the major principal axis. The ratio of the expansion coefficients satisfies the relation

$$\frac{\gamma_i}{\beta_i} = -\frac{c}{a - \mu_i v} = -\frac{d - \mu_i v}{b}. \quad (15)$$

The relationship between eigenvectors  $\zeta_i$ , the flow velocity  $v$ , and the vector  $\omega$  is illustrated in Figure 1. The cosine of the angle  $\Phi$  between  $v$  and  $\zeta_1$ , taken as the major principal axis of the dispersion ellipsoid, is given by

$$\cos \Phi = \frac{v \cdot \zeta_1}{v} = \frac{\gamma_1 v}{\sqrt{\gamma_1^2 v^2 + \beta_1^2 \omega^2}}. \quad (16)$$

The angle  $\Phi$  depends on the fluid velocity and its angle with the axis of symmetry, in addition to material properties of the porous medium. If the coefficients  $b$  and  $c$  vanish, it is clear from equations (11a) and (11b) that vectors  $v$  and  $\omega$  are eigenvectors of  $D$  with eigenvalues  $a$  and  $d$ , respectively, and the angle  $\Phi$  vanishes. Thus in this case the major principal axis corresponds to the direction of flow. For this to occur the coefficients  $\alpha_3$  and  $\alpha_4$  must be related by the expression

$$\alpha_4 = -2 \cos \theta \alpha_3 = -2 \frac{\lambda \cdot v}{v} \alpha_3. \quad (17)$$

In addition,  $\Phi$  always vanishes for flow parallel to the symmetry axes ( $\cos \theta = 1, \omega = 0$ ). For flow perpendicular to the symmetry axis,  $v$  and  $\omega$  are not eigenvectors unless  $\alpha_4 = 0$ . It should be noted that according to equation (17),  $\alpha_4$  can become negative. However, the physically meaningful quantities are the eigenvalues of  $D$  which must be nonnegative.

[15] It is not surprising that the general form of the dispersion tensor as given by equation (3) allows for principal axes not aligned with the direction of flow. Indeed, the form of the dispersion tensor is not in any way restricted to a description of dispersion, but is simply the most general mathematical form for a tensor that obeys proper transformation rules which can be constructed from two vectors. There is some precedent for  $\Phi \neq 0$  in heterogeneous porous media [de Marsily, 1986, p. 250]. Both Gelhar and Axness [1983] and Neuman *et al.* [1987] have demonstrated theoretically that in general  $\Phi \neq 0$ , based on a stochastic analysis of transport in heterogeneous media. However, there is disagreement between the authors on the sign of the angle  $\Phi$ . At present there does not exist experimental or field confirmation of the situation when  $\Phi \neq 0$ , which appears difficult at best to establish.

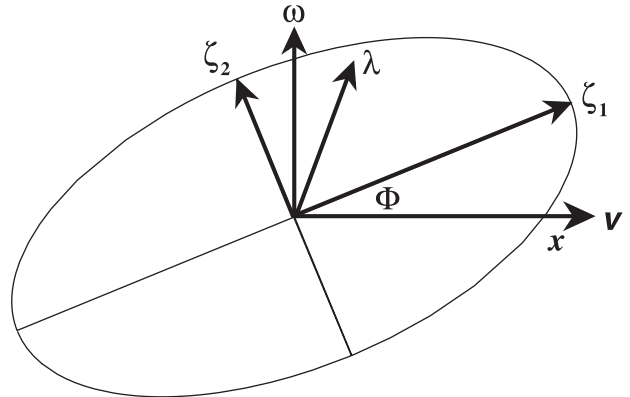


**Figure 1.** Illustration of the relation between the eigenvectors of  $D$ , the symmetry axis  $\lambda$ , the vector  $\omega$ , and the fluid velocity  $v$  for a general axisymmetric medium.

[16] If equation (17) holds so that one of the principal axes is aligned with the direction of flow, then equations (11a) and (11b) reduce to the simpler forms

$$D \cdot v = [\alpha_1 + \alpha_2 + \cos^2 \theta \alpha_3] v v = \alpha_L v v, \quad (18a)$$

and

$$D \cdot \omega = [\alpha_1 + (1 - \cos^2 \theta) \alpha_3] v \omega = \alpha_T v \omega, \quad (18b)$$

indicating that both  $v$  and  $\omega$  are eigenvectors of  $D$  with longitudinal and transverse dispersivities given by

$$\alpha_L = \alpha_1 + \alpha_2 + \cos^2 \theta \alpha_3, \quad (19a)$$

and

$$\alpha_T = \alpha_1 + (1 - \cos^2 \theta) \alpha_3, \quad (19b)$$

respectively. Thus when  $\theta = \pi/2$ ,  $\alpha_L = \alpha_T^H = \alpha_1 + \alpha_2$ , and  $\alpha_T = \alpha_T^V = \alpha_1 + \alpha_3$ . When  $\theta = 0$ ,  $\alpha_L = \alpha_T^H = \alpha_1 + \alpha_2 + \alpha_3$  and  $\alpha_T = \alpha_T^V = \alpha_1$ .

[17] It is interesting to note that in the case when equation (17) holds, the eigenvectors of  $D$  are independent of the coefficients  $\alpha_i$ . Solving for the  $\alpha_i$  yields the inverse relations

$$\alpha_1 = \alpha_T^H, \quad (20a)$$

$$\alpha_2 = \alpha_L - \alpha_T^H - \frac{\cos^2 \theta}{1 - \cos^2 \theta} (\alpha_T - \alpha_T^H), \quad (20b)$$

$$\alpha_3 = \frac{\alpha_T - \alpha_T^H}{1 - \cos^2 \theta}. \quad (20c)$$

With these results the dispersion tensor can be written in dyadic form as

$$D = \alpha_T^H v I + \left[ \alpha_L - \alpha_T^H + \frac{\cos^2 \theta}{1 - \cos^2 \theta} (\alpha_T - \alpha_T^H) \right] \frac{v v}{v} + \frac{\alpha_T - \alpha_T^H}{1 - \cos^2 \theta} \cdot v \left[ \lambda \lambda - \frac{\cos \theta}{v} (\lambda v + v \lambda) \right], \quad (21)$$

and in terms of  $\mathbf{v}$  and  $\omega$  as

$$\mathbf{D} = \alpha_T^H \mathbf{v} \mathbf{I} + (\alpha_L - \alpha_T^H) \frac{\mathbf{v}\mathbf{v}}{v} + \frac{\alpha_T - \alpha_T^H}{1 - \cos^2\theta} v \omega \omega. \quad (22)$$

The longitudinal and transverse dispersivities,  $\alpha_L$  and  $\alpha_T$ , defined as the eigenvalues of  $\mathbf{v}$  and  $\omega$ , respectively, can be arbitrary functions of the scalar quantities  $v$  and  $\cos \theta$ . Whether or not this four parameter representation of the dispersion tensor provides an adequate description for flow at an angle to the symmetry axis needs to be verified by direct comparison with field observations.

#### 2.4. Special Cases

[18] In this section special cases corresponding to an isotropic medium, and an axisymmetric medium with flow parallel and perpendicular to the symmetry axis are considered in more detail.

##### 2.4.1. Isotropic media

[19] For the special case of an isotropic medium,  $\lambda = \mathbf{0}$  since there is no preferred axis of symmetry, and it follows that the general form of the dispersion tensor reduces to the well-known form [Poreh, 1965; Dagan, 1984]

$$\mathbf{D} = \alpha_1 v \mathbf{I} + \alpha_2 \frac{\mathbf{v}\mathbf{v}}{v}. \quad (23)$$

To relate the coefficients  $\alpha_1$  and  $\alpha_2$  to the usual longitudinal and transverse dispersivity coefficients  $\alpha_L$  and  $\alpha_T$ , note that  $\mathbf{v}$  is an eigenvector of  $\mathbf{D}$  with eigenvalue  $\alpha_1 + \alpha_2$ , i.e.

$$\mathbf{D} \cdot \mathbf{v} = (\alpha_1 + \alpha_2) v \mathbf{v}. \quad (24)$$

Thus it follows that  $\alpha_L = \alpha_1 + \alpha_2$ . The remaining two eigenvectors represented by  $\zeta_i$ , orthogonal to  $\mathbf{v}$ , belong to the degenerate eigenvalue  $\alpha_1 v$ . Hence it follows that

$$\mathbf{D} \cdot \zeta_i = \alpha_1 v \zeta_i. \quad (25)$$

Thus  $\alpha_T = \alpha_1$ , giving  $\alpha_2 = \alpha_L - \alpha_T$ . The resulting dispersion tensor for an isotropic porous medium has the form [Bear, 1972]

$$\begin{aligned} \mathbf{D} &= \alpha_T v \mathbf{I} + (\alpha_L - \alpha_T) \frac{\mathbf{v}\mathbf{v}}{v}, \\ &= \begin{pmatrix} \alpha_T v + (\alpha_L - \alpha_T) \frac{v_1^2}{v} & (\alpha_L - \alpha_T) \frac{v_1 v_2}{v} & (\alpha_L - \alpha_T) \frac{v_1 v_3}{v} \\ (\alpha_L - \alpha_T) \frac{v_2 v_1}{v} & \alpha_T v + (\alpha_L - \alpha_T) \frac{v_2^2}{v} & (\alpha_L - \alpha_T) \frac{v_2 v_3}{v} \\ (\alpha_L - \alpha_T) \frac{v_3 v_1}{v} & (\alpha_L - \alpha_T) \frac{v_3 v_2}{v} & \alpha_T v + (\alpha_L - \alpha_T) \frac{v_3^2}{v} \end{pmatrix}. \end{aligned} \quad (26)$$

##### 2.4.2. Axisymmetric medium: Flow parallel to symmetry axis

[20] For an axisymmetric medium with flow along the axis of symmetry it follows that

$$\mathbf{v} = v \boldsymbol{\lambda}, \quad (27)$$

$\omega = \mathbf{0}$ , and  $\mathbf{D}$  becomes

$$\mathbf{D} = \alpha_1 v \mathbf{I} + (\alpha_2 + \alpha_3 + \alpha_4) v \boldsymbol{\lambda} \boldsymbol{\lambda}. \quad (28)$$

It is apparent that  $\mathbf{v}$  (and  $\boldsymbol{\lambda}$ ) is an eigenvector belonging to the eigenvalue  $(\alpha_1 + \alpha_2 + \alpha_3 + \alpha_4)v$ , and the eigenvalue  $\alpha_1 v$  is degenerate with eigenvectors in the plane normal to  $\boldsymbol{\lambda}$ .

[21] Introducing the notation  $\alpha_L^V$  for longitudinal dispersivity along the axis of symmetry, and  $\alpha_T^H$  for horizontal transverse dispersivity, the dispersion tensor can be written as

$$\mathbf{D} = \alpha_T^H v \mathbf{I} + (\alpha_L^V - \alpha_T^H) \frac{\mathbf{v}\mathbf{v}}{v}, \quad (29)$$

with  $\alpha_1 = \alpha_T^H$  and  $\alpha_2 + \alpha_3 + \alpha_4 = \alpha_L^V - \alpha_T^H$ . This form of the dispersion tensor has the same form as that for an isotropic medium. Thus  $\mathbf{v}$  is a principal direction of the dispersion tensor satisfying

$$\mathbf{D} \cdot \mathbf{v} = \alpha_L^V v \mathbf{v}, \quad (30)$$

with

$$\alpha_L^V = \alpha_1 + \alpha_2 + \alpha_3 + \alpha_4. \quad (31)$$

The remaining two eigenvectors are orthogonal to  $\mathbf{v}$  but otherwise arbitrary, belonging to the degenerate eigenvalue  $\alpha_{TV}^H$ .

##### 2.4.3. Axisymmetric medium: Flow perpendicular to symmetry axis

[22] For the special case when  $\mathbf{v}$  and  $\boldsymbol{\lambda}$  are orthogonal ( $\boldsymbol{\lambda} = \omega$ ), and  $\cos \theta = 0$ , it follows that

$$\mathbf{D} \cdot \mathbf{v} = (\alpha_1 + \alpha_2) v \mathbf{v} + \frac{1}{2} \alpha_4 v^2 \boldsymbol{\lambda}, \quad (32a)$$

and

$$\mathbf{D} \cdot \boldsymbol{\lambda} = \frac{1}{2} \alpha_4 \mathbf{v} + (\alpha_1 + \alpha_3) v \boldsymbol{\lambda}. \quad (32b)$$

From these relations it is apparent that, in general, neither  $\mathbf{v}$  nor  $\boldsymbol{\lambda}$  are eigenvectors of  $\mathbf{D}$  unless  $\alpha_4 = 0$ , in which case both vectors  $\mathbf{v}$  and  $\boldsymbol{\lambda}$  are eigenvectors satisfying the eigenvalue equations

$$\begin{aligned} \mathbf{D} \cdot \mathbf{v} &= (\alpha_1 + \alpha_2) v \mathbf{v}, \\ &= \alpha_L^H v \mathbf{v}, \end{aligned} \quad (33a)$$

and

$$\begin{aligned} \mathbf{D} \cdot \boldsymbol{\lambda} &= (\alpha_1 + \alpha_3) v \boldsymbol{\lambda}, \\ &= \alpha_T^V v \boldsymbol{\lambda}. \end{aligned} \quad (33b)$$

In this case there are two transverse dispersivities, horizontal and vertical, denoted by  $\alpha_T^V$  and  $\alpha_T^H$ . Longitudinal dispersivity is denoted by  $\alpha_L^H$ , because in general it may be different from  $\alpha_L^T$  for flow in the direction parallel to  $\boldsymbol{\lambda}$ .

[23] Noting that  $\mathbf{v} \times \boldsymbol{\lambda}$  is an eigenvector belonging to the eigenvalue  $\alpha_1$  which may be identified with  $\alpha_T^H$ , it follows that

$$\alpha_1 = \alpha_T^H, \quad (34a)$$

$$\alpha_2 = \alpha_L^H - \alpha_T^H, \quad (34b)$$

and

$$\alpha_3 = \alpha_T^V - \alpha_T^H. \quad (34c)$$

[24] For flow perpendicular to the axis of symmetry and assuming  $\alpha_4$  is sufficiently small, it follows that the angle of inclination of the principal axis to the direction of flow is given approximately by the relation

$$\cos \Phi \simeq \frac{1}{\sqrt{1 + \frac{\alpha_4^2}{4(\alpha_2 - \alpha_3)^2}}} \simeq 1 - \frac{\alpha_4^2}{8(\alpha_2 - \alpha_3)^2}, \quad (35)$$

or

$$\Phi \simeq \frac{\alpha_4^2}{4(\alpha_2 - \alpha_3)^2}. \quad (36)$$

Generally,  $\alpha_2 \gg \alpha_3$  since  $\alpha_2$  involves the difference between longitudinal and transverse diffusivities, whereas  $\alpha_3$  is proportional to the difference in transverse diffusivities.

## 2.5. New Form of the Dispersion Tensor for Axisymmetric Media

[25] To construct an alternative form of the dispersion tensor which could apply to flow at any arbitrary angle to the axis of symmetry, and still honor tensorial transformation properties, the appropriate functional form of the coefficients  $\alpha_L$  and  $\alpha_T$  in equation (21) or (22) on the direction of flow must be determined. Two limiting cases must be met for flow parallel and perpendicular to the axis of symmetry. For flow parallel to the symmetry axis longitudinal dispersion should reduce to the vertical longitudinal dispersivity  $\alpha_L^V$ , and transverse dispersion should be isotropic with dispersivity described by  $\alpha_T^V$ . For flow perpendicular to the axis of symmetry, longitudinal dispersion should reduce to the horizontal longitudinal dispersivity  $\alpha_L^H$ , with transverse dispersion described by the two coefficients,  $\alpha_T^V$  and  $\alpha_T^H$ . Clearly it is not possible to deduce a priori the form of the dispersion tensor for flow at an angle to the symmetry axis without additional information. It would be expected that the dispersion tensor would depend on the specific properties of the porous medium, and even head differences. Without additional information it is assumed that the longitudinal and transverse dispersivities have the forms

$$\alpha_L = \mathcal{G}_L(\cos \theta; \alpha_L^V, \alpha_L^H), \quad (37a)$$

and

$$\alpha_T = \mathcal{G}_T(\cos \theta; \alpha_T^V, \alpha_T^H), \quad (37b)$$

where the only dependence is on the scalar  $\cos \theta$  in addition to the dispersivity parameters. The functions  $\mathcal{G}_{L,T}$  satisfy the end-member conditions

$$\mathcal{G}_L(0; \alpha_L^V, \alpha_L^H) = \alpha_L^V, \quad (\text{vertical flow}), \quad (38a)$$

$$\mathcal{G}_T(0; \alpha_T^V, \alpha_T^H) = \alpha_T^H, \quad (\text{vertical flow}), \quad (38b)$$

$$\mathcal{G}_L(1; \alpha_L^V, \alpha_L^H) = \alpha_L^H, \quad (\text{horizontal flow}), \quad (38c)$$

$$\mathcal{G}_T(1; \alpha_T^V, \alpha_T^H) = \alpha_T^V, \quad (\text{horizontal flow}), \quad (38d)$$

but are otherwise arbitrary. To determine the functional form of  $\mathcal{G}_{L,T}$  it would be necessary to compare predictions based

on a specific form of the dispersion tensor with actual field observations, or to carry out numerical experiments involving heterogeneous media.

[26] For the new form of the dispersion tensor proposed here, the following dependency on  $\cos \theta$  is chosen

$$\mathcal{G}_L = \alpha_L^H + \cos^2 \theta (\alpha_L^V - \alpha_L^H), \quad (39a)$$

and

$$\mathcal{G}_T = \alpha_T^V + \cos^2 \theta (\alpha_T^H - \alpha_T^V). \quad (39b)$$

With this choice of  $\mathcal{G}_{L,T}$ , the desired behavior is obtained that is at least correct for the end-member cases of flow parallel and perpendicular to the axis of symmetry. However, clearly an infinite number of functional forms are possible which satisfy conditions (38a), (38b), (38c), and (38d). In what follows it is assumed that the transverse horizontal dispersivity  $\alpha_T^H$  has the same value for flow parallel and perpendicular to the axis of symmetry. However, it is not apparent that this necessarily must be the case, which would complicate the formulation.

[27] To obtain expressions for the coefficients  $\alpha_i$  in terms of the set  $\alpha_L^V$ ,  $\alpha_L^H$ ,  $\alpha_T^V$ , and  $\alpha_T^H$ , the expressions for longitudinal and transverse dispersion given by equations (19a) and (19b) are equated to the desired forms given by

$$\begin{aligned} \alpha_L &= \alpha_1 + \alpha_2 - \cos^2 \theta \alpha_3, \\ &= \alpha_L^H + \cos^2 \theta (\alpha_L^V - \alpha_L^H), \end{aligned} \quad (40a)$$

and

$$\begin{aligned} \alpha_T &= \alpha_1 + (1 - \cos^2 \theta) \alpha_3, \\ &= \alpha_T^V + \cos^2 \theta (\alpha_T^H - \alpha_T^V), \end{aligned} \quad (40b)$$

As can be seen from these relations, the eigenvalue for longitudinal dispersion varies between the horizontal and vertical longitudinal dispersivities as the flow direction varies from perpendicular to parallel to the symmetry axis of the medium. Similarly, the eigenvalue for transverse dispersivity varies between the vertical and horizontal transverse dispersivities.

[28] The coefficient  $\alpha_1$  is assumed to be given by

$$\alpha_1 = \alpha_T^H, \quad (41)$$

independent of the direction of the flow velocity relative to the symmetry axis. This is reasonable because the eigenvector  $\mathbf{v} \times \boldsymbol{\omega}$  is always perpendicular to the symmetry axis  $\mathbf{x}$  and the flow velocity  $\mathbf{v}$  with eigenvalue  $\alpha_1 v$ , and hence it should only reflect horizontal transverse dispersion. Equations (40a) and (40b) provide two equations for the two coefficients  $\alpha_2$  and  $\alpha_3$ . It follows that

$$\begin{aligned} \alpha_2 &= \alpha_L^H - \alpha_T^H + \cos^2 \theta (\alpha_L^V - \alpha_L^H + \alpha_T^V - \alpha_T^H), \\ &= \alpha_L - \alpha_T + \alpha_T^V - \alpha_T^H, \end{aligned} \quad (42)$$

and

$$\alpha_3 = \alpha_T^V - \alpha_T^H, \quad (43)$$

with  $\alpha_4$  given by equation (17). The corresponding eigenvalues for eigenvectors  $\mathbf{v}$  and  $\omega$  are given, respectively, by

$$\mathbf{D} \cdot \mathbf{v} = [\alpha_L^H + \cos^2\theta(\alpha_L^V - \alpha_L^H)]\mathbf{v}\mathbf{v}, \quad (44a)$$

and

$$\mathbf{D} \cdot \omega = [\alpha_T^V + \cos^2\theta(\alpha_T^H - \alpha_T^V)]\mathbf{v}\omega, \quad (44b)$$

defining the longitudinal and transverse dispersion coefficients  $\alpha_L$  and  $\alpha_T$  according to equations (40a) and (40b). The dispersion tensor has the form

$$\begin{aligned} \mathbf{D} = & \alpha_T^H \mathbf{v} \mathbf{I} + [\alpha_L^H - \alpha_T^H + \cos^2\theta(\alpha_L^V - \alpha_L^H + \alpha_T^V - \alpha_T^H)] \frac{\mathbf{v}\mathbf{v}}{v} \\ & + (\alpha_T^V - \alpha_T^H)v \left[ \boldsymbol{\lambda} \boldsymbol{\lambda} - \frac{\cos\theta}{v} (\boldsymbol{\lambda}\mathbf{v} + \mathbf{v}\boldsymbol{\lambda}) \right], \end{aligned} \quad (45)$$

or in terms of  $\omega$

$$\mathbf{D} = \alpha_T^H \mathbf{v} \mathbf{I} + [\alpha_L^H - \alpha_T^H + \cos^2\theta(\alpha_L^V - \alpha_L^H)] \frac{\mathbf{v}\mathbf{v}}{v} + (\alpha_T^V - \alpha_T^H)v\omega\omega. \quad (46)$$

In terms of individual matrix elements with  $\boldsymbol{\lambda} = (0, 0, 1)$ , the dispersion tensor becomes

$$D_{11} = \alpha_L \frac{v_1^2}{v} + \alpha_T^H \frac{v_2^2}{v} \left( 1 + \frac{v_3^2}{v_1^2 + v_2^2} \right) + \alpha_T \frac{v_3^2}{v} \frac{v_1^2}{v_1^2 + v_2^2}, \quad (47a)$$

$$D_{22} = \alpha_T^H \frac{v_1^2}{v} \left( 1 + \frac{v_3^2}{v_1^2 + v_2^2} \right) + \alpha_L \frac{v_2^2}{v} + \alpha_T \frac{v_3^2}{v} \frac{v_2^2}{v_1^2 + v_2^2}, \quad (47b)$$

$$D_{33} = \alpha_T \frac{(v_1^2 + v_2^2)}{v} + \alpha_L \frac{v_3^2}{v}, \quad (47c)$$

$$D_{12} = \left[ \alpha_L - \alpha_T^H \left( 1 + \frac{v_3^2}{v_1^2 + v_2^2} \right) + \alpha_T \frac{v_3^2}{v_1^2 + v_2^2} \right] \frac{v_1 v_2}{v}, \quad (47d)$$

$$D_{13} = (\alpha_L - \alpha_T) \frac{v_1 v_3}{v}, \quad (47e)$$

$$D_{23} = (\alpha_L - \alpha_T) \frac{v_2 v_3}{v}. \quad (47f)$$

In these relations  $\alpha_T$  and  $\alpha_L$  are functions of  $\cos\theta$  as given by equations (40a) and (40b).

[29] According to this formulation, the dispersion tensor can be expressed in terms of the four dispersivity coefficients  $\alpha_L^{VH}$  and  $\alpha_T^{VH}$ . By appropriately choosing  $\alpha_4$ , one of the principal axes can always be lined up with the direction of flow. Only through comparison with field data will it be possible to determine the correct form of the coefficients  $\alpha_i$  in terms of the invariants  $\theta$  and  $v$ .

[30] In principle, at the laboratory scale the coefficients  $\alpha_L^H$ ,  $\alpha_L^V$ ,  $\alpha_T^H$ , and  $\alpha_T^V$  could be estimated by conducting experiments on suitably oriented cores. One approach would be to estimate  $\alpha_L^H$  and  $\alpha_L^V$  by measuring tracer

breakthrough curves on a core sample oriented normal and parallel, respectively, to the axis of symmetry. Transverse dispersivities  $\alpha_T^H$ ,  $\alpha_T^V$  could then be estimated by performing 2-dimensional flow experiments on rock slabs, for example. Such results would be of significant theoretical interest. However, it is well known that dispersivity values are a strong function of scale, hence it is necessary to estimate the dispersivity coefficients at a larger scale using field experiments. In the most general flow situation, the coefficients  $\alpha_1$ ,  $\alpha_2$ ,  $\alpha_3$ , and  $\alpha_4$  could be estimated from field data using a numerical model in conjunction with nonlinear parameter estimation by fitting an observed three dimensional plume. If a tracer test can be conducted in a portion of the aquifer where the fluid velocity is unidirectional and horizontal coinciding with the principal axis of the dispersion tensor (as often is the case), the parameter estimation procedure can be simplified considerably. In this case, the dispersion tensor simplifies to

$$D_{11} = \alpha_L^H v, \quad D_{22} = \alpha_T^H v, \quad D_{33} = \alpha_T^V v, \quad (48)$$

with zero off-diagonal terms. With appropriately spaced observation wells, the coefficients  $\alpha_L^H$ ,  $\alpha_T^H$ , and if enough 3-dimensional information is available,  $\alpha_T^V$  as well, can be estimated. Note that in this particular case, no information is available about  $\alpha_L^V$ . To obtain this coefficient, another test would have to be conducted in a portion of the field where the fluid velocity has a significant vertical component. If the spread of a plume can be measured in such a case, then equations (47a), (47b), (47c), (47d), (47e), and (47f) can be used to estimate the value of the coefficient  $\alpha_L^V$ , and perhaps  $\alpha_T^V$ . Once the dispersivities are estimated for horizontal and vertical flow, the  $\theta$  dependence of the dispersivity coefficients for flow at an angle to the symmetry axis could be tested.

## 2.6. Comparison With Dispersion Tensor Proposed by Burnett and Frind [1987]

[31] Burnett and Frind [1987] proposed a simplified form of the dispersion tensor for axisymmetric media, hereafter designated as  $\mathbf{D}_{BF}$  and referred as the BF-dispersion tensor. The BF-dispersion tensor involves only three independent parameters. These refer to longitudinal dispersion ( $\alpha_L$ ), and transverse horizontal ( $\alpha_T^H$ ) and vertical ( $\alpha_T^V$ ) dispersion. Burnett and Frind [1987] derived the form of the dispersion tensor by generalizing the form for isotropic media to account for different transverse dispersivities in the horizontal and vertical directions as observed in natural stratified media with flow along the bedding plane [Anderson, 1979; Robson, 1978]. For example, Zheng and Bennett [1995, pp. 45–46] have used the Burnett-Frind tensor to model dispersion in axisymmetric media.

[32] Burnett and Frind [1987] write the dispersion tensor as a matrix of coefficients in the form

$$\mathbf{D}_{BF} = \begin{pmatrix} \alpha_L \frac{v_1^2}{v} + \alpha_T^H \frac{v_2^2}{v} + \alpha_T^V \frac{v_3^2}{v} & (\alpha_L - \alpha_T^H) \frac{v_1 v_2}{v} & (\alpha_L - \alpha_T^V) \frac{v_1 v_3}{v} \\ (\alpha_L - \alpha_T^H) \frac{v_2 v_1}{v} & \alpha_T^H \frac{v_1^2}{v} + \alpha_L \frac{v_2^2}{v} + \alpha_T^V \frac{v_3^2}{v} & (\alpha_L - \alpha_T^V) \frac{v_2 v_3}{v} \\ (\alpha_L - \alpha_T^V) \frac{v_3 v_1}{v} & (\alpha_L - \alpha_T^V) \frac{v_3 v_2}{v} & \alpha_T^V \frac{v_1^2 + v_2^2}{v} + \alpha_L \frac{v_3^2}{v} \end{pmatrix}. \quad (49)$$

The diagonal elements may be written in a form similar to the isotropic case given in equation (26) as

$$(D_{\text{BF}})_{11} = \alpha_T^H v + (\alpha_L - \alpha_T^H) \frac{v_1^2}{v} + (\alpha_T^V - \alpha_T^H) \frac{v_3^2}{v}, \quad (50\text{a})$$

$$(D_{\text{BF}})_{22} = \alpha_T^H v + (\alpha_L - \alpha_T^H) \frac{v_2^2}{v} + (\alpha_T^V - \alpha_T^H) \frac{v_3^2}{v}, \quad (50\text{b})$$

$$(D_{\text{BF}})_{33} = \alpha_T^V v + (\alpha_L - \alpha_T^V) \frac{v_2^3}{v}. \quad (50\text{c})$$

It remains to prove whether in fact this matrix actually forms a tensor in the strict sense of the word in that it satisfies the appropriate transformation properties upon a change of coordinate system.

[33] To determine the tensorial properties of the BF-dispersion tensor, it is first noted that  $\mathbf{D}_{\text{BF}}$  must be interpreted as referring to a particular coordinate system in which the symmetry axis of the medium lies along the  $z$ -axis:  $\lambda = (0, 0, 1)$ . Then  $v_3$  can be written as the scalar product  $v_3 = v \cos \theta = \lambda \cdot v$ . With this in mind, the matrix  $\mathbf{D}_{\text{BF}}$  can be expressed as

$$\begin{aligned} \mathbf{D}_{\text{BF}} = & [\alpha_T^H + \cos^2 \theta (\alpha_T^V - \alpha_T^H)] v \mathbf{I} + (\alpha_L - \alpha_T^H) \frac{v \mathbf{w}}{v} \\ & + (\alpha_T^V - \alpha_T^H) v \left[ \lambda \lambda - \frac{\cos \theta}{v} (\lambda v + v \lambda) \right], \end{aligned} \quad (51)$$

valid for any orientation of the coordinate system relative to the symmetry axis. Accordingly,  $\mathbf{D}_{\text{BF}}$  is a tensor by construction. Comparing equation (51) with equation (3) leads to the following identification of the coefficients  $\alpha_i$

$$\alpha_1 = \alpha_T^H + \cos^2 \theta (\alpha_T^V - \alpha_T^H), \quad (52\text{a})$$

$$\alpha_2 = \alpha_L - \alpha_T^H, \quad (52\text{b})$$

$$\alpha_3 = \alpha_T^V - \alpha_T^H, \quad (52\text{c})$$

and

$$\alpha_4 = -2 \cos \theta (\alpha_T^V - \alpha_T^H) = -2 \cos \theta \alpha_3. \quad (52\text{d})$$

It follows that equation (17) is satisfied for the BF-dispersion tensor and thus both  $\mathbf{v}$  and  $\omega$  are eigenvectors belonging to eigenvalues  $\alpha_L v$  and  $\alpha_T^V v$ , respectively, according to equations (18a) and (18b):

$$\mathbf{D}_{\text{BF}} \cdot \mathbf{v} = \alpha_L v \mathbf{v}, \quad (53\text{a})$$

and

$$\mathbf{D}_{\text{BF}} \cdot \omega = \alpha_T^V v \omega. \quad (53\text{b})$$

The eigenvector  $\zeta_3$ , orthogonal to  $\mathbf{v}$  and  $\omega$ , belongs to the eigenvalue  $\alpha_1$

$$\mathbf{D}_{\text{BF}} \cdot \zeta_3 = [\alpha_T^H + \cos^2 \theta (\alpha_T^V - \alpha_T^H)] v \zeta_3. \quad (53\text{c})$$

Note, however, that the BF-tensor, even though it transforms as a tensor, does not satisfy conditions (38a), (38b), (38c), and (38d).

[34] For flow perpendicular to the axis of symmetry, the BF-tensor agrees with the more general form. And for small  $v_3$ , the generalized form of the dispersion tensor reduces to the form given by *Burnett and Frind* [1987].

[35] However, there are several problems with the form of the BF-dispersion tensor. The relation given in equation (41) differs from that of  $\mathbf{D}_{\text{BF}}$  given in equation (52a) in which  $\alpha_1$  is a function of  $\cos \theta$ . The relation for  $\alpha_2$  is different from that obtained for the BF-dispersion tensor given in equation (52b), but reduces to the Burnett-Frind value for flow perpendicular to the axis of symmetry ( $\cos \theta = 0$  with  $\alpha_L = \alpha_L^H$ ). As the direction of  $v$  varies from parallel ( $\cos \theta = 1$ ) to perpendicular ( $\cos \theta = 0$ ) to  $\lambda$ ,  $\alpha_1$  varies between  $\alpha_T^V$  and  $\alpha_T^H$ . This behavior is not correct because the vector  $\zeta_3$  always remains perpendicular to the symmetry axis and the direction of flow, and hence the eigenvalue  $\alpha_1$  should always be equal to the horizontal transverse dispersivity. In addition, for the BF-dispersion tensor the transverse dispersivity corresponding to the eigenvector  $\omega$  is independent of the direction of flow and always equal to the vertical transverse dispersivity. However, it is this eigenvalue which should vary from transverse vertical to transverse horizontal as the vectors  $v$  and  $\omega$  range from perpendicular to parallel. These apparent deficiencies of the BF-dispersion tensor are corrected in the next section by introducing a new form of the dispersion tensor for axisymmetric media.

[36] As noted in the previous section, a drawback of the BF-dispersion tensor is that the transverse dispersivity along the principal axis  $\omega$  is independent of the direction of flow and given by the vertical transverse dispersivity. Intuitively, this would seem correct only for flow perpendicular to the symmetry axis, taken as pointing in the vertical direction. For flow along the symmetry axes, or at some angle to it, it would be expected that the transverse dispersivity should reflect the angle of flow to the symmetry axis. In addition, for the BF-dispersion tensor there is only one coefficient for longitudinal dispersion which is therefore the same for flow in both the vertical and horizontal directions, i.e., parallel and perpendicular to the axis of symmetry, contrary to what one would expect for nonisotropic porous media.

### 3. Particle Tracking Implementation

[37] Random-walk particle tracking algorithms present an attractive technique to implement the dispersion tensor in axisymmetric media, due to their relatively simple mathematical formulation and ability to capture sharp fronts without significant numerical error. In the limit of a large number of particles, the particle density distribution reproduces the continuum-based mass conservation equation. The expression for the particle trajectory is comprised of a deterministic component that depends only on the local velocity field, and a stochastic term that describes dispersion via a random-walk method. In finite difference form the particle trajectory is obtained from the equation

$$\mathbf{X}_n = \mathbf{X}_{n-1} + \Delta t_n \mathbf{A}_{n-1} + \sqrt{\Delta t_n} \mathbf{B}_{n-1} \mathbf{Z}. \quad (54)$$

written in matrix form for a time step  $\Delta t_n$ , where  $\mathbf{Z}$  represents a random vector and  $\mathbf{X}_n$  denotes the displacement

vector after  $n$  steps. This equation is referred to as the Langevin equation. The displacement matrix  $\mathbf{B}$  and the drift term  $\mathbf{A}$  can be related to the dispersion tensor  $\mathbf{D}$ , flow field  $\mathbf{v}$ , and porosity  $\phi$  through the Fokker-Planck equation as demonstrated in Appendix A. There it is demonstrated that the displacement matrix  $\mathbf{B}$  is related to the dispersion tensor by the expression

$$\mathbf{B}\tilde{\mathbf{B}} = 2\mathbf{D}. \quad (55)$$

As demonstrated in Appendix A, this relation can be solved for the displacement matrix  $\mathbf{B}$  yielding

$$\mathbf{B} = \sqrt{2}\mathbf{U}\mathbf{Q}, \quad (56)$$

where  $\mathbf{U}$  represents an orthogonal transformation that diagonalizes  $\mathbf{D}$ , and the matrix  $\mathbf{Q}$  denotes the matrix composed of the square root of the eigenvalues of  $\mathbf{D}$ . The uniqueness of  $\mathbf{B}$  and  $\mathbf{U}$  is investigated in Appendix B. The background drift term  $\mathbf{A}$  given by

$$\mathbf{A} = \mathbf{v} + \frac{1}{\phi} \nabla \cdot \phi \mathbf{D}, \quad (57)$$

involves not just the pore velocity  $\mathbf{v}$ , but also contains contributions from the divergence of the dispersion tensor and gradient of the porosity. The spatial dependence of the dispersion tensor occurs through the velocity field and possibly at boundaries at which changes in material properties occur leading to differences in dispersivity and porosity across such boundaries. *Kinzelbach and Uffink* [1991] noted that the contribution  $\nabla \cdot \mathbf{D}$  can be significant at stagnation points in the flow field where a rapid change in velocity exists. *LaBolle et al.* [1996] investigated the effects of material boundaries on this term and the importance of including it in particle tracking algorithms. In section 4.5 a comparison is made with and without this term present for a steady but spatially variable flow field and it is demonstrated that this term is essential to obtain correct results.

[38] For an arbitrary axisymmetric medium, the orthogonal transformation  $\mathbf{U}$  is given by

$$\mathbf{U} = \left( \frac{\gamma_1 \mathbf{v} + \beta_1 \boldsymbol{\omega}}{\sqrt{\gamma_1^2 v^2 + \beta_1^2 \omega^2}}, \frac{\gamma_2 \mathbf{v} + \beta_2 \boldsymbol{\omega}}{\sqrt{\gamma_2^2 v^2 + \beta_2^2 \omega^2}}, \frac{\mathbf{v} \times \boldsymbol{\omega}}{\sqrt{(\mathbf{v} \times \boldsymbol{\omega}) \cdot (\mathbf{v} \times \boldsymbol{\omega})}} \right). \quad (58)$$

For the special case in which one of the principal axes is parallel to the fluid velocity,  $\mathbf{U}$  becomes

$$\mathbf{U} = \left( \frac{\mathbf{v}}{v}, \frac{\boldsymbol{\omega}}{\omega}, \frac{\mathbf{v} \times \boldsymbol{\omega}}{\sqrt{(\mathbf{v} \times \boldsymbol{\omega}) \cdot (\mathbf{v} \times \boldsymbol{\omega})}} \right). \quad (59)$$

Writing

$$\mathbf{U} = \begin{pmatrix} U_{11} & U_{12} & U_{13} \\ U_{21} & U_{22} & U_{23} \\ U_{31} & U_{32} & U_{33} \end{pmatrix}, \quad (60)$$

the displacement matrix  $\mathbf{B}$  is given by

$$\mathbf{B} = \begin{pmatrix} U_{11} \sqrt{2(\mu_1 v + D_0)} & U_{12} \sqrt{2(\mu_2 v + D_0)} & U_{13} \sqrt{2(\alpha_1 v + D_0)} \\ U_{21} \sqrt{2(\mu_1 v + D_0)} & U_{22} \sqrt{2(\mu_2 v + D_0)} & U_{23} \sqrt{2(\alpha_1 v + D_0)} \\ U_{31} \sqrt{2(\mu_1 v + D_0)} & U_{32} \sqrt{2(\mu_2 v + D_0)} & U_{33} \sqrt{2(\alpha_1 v + D_0)} \end{pmatrix}, \quad (61)$$

where  $D_0$  denotes the effective molecular diffusion coefficient. For the general case of flow oblique to the symmetry axis, the transformation matrix  $\mathbf{U}$ , and hence  $\mathbf{B}$ , are unique since the dispersion tensor  $\mathbf{D}$  has a nondegenerate set of eigenvalues. This formulation breaks down, however, when flow occurs along the symmetry axis since then  $\boldsymbol{\omega} = \mathbf{0}$  and the cross product vanishes. In this case the matrix  $\mathbf{U}$  is not unique since there are two degenerate eigenvalues. *Tompson et al.* [1987] exploited this non-uniqueness to obtain a nonsingular representation for  $\mathbf{U}$ .

[39] In the axisymmetric case, the eigenvalues of the dispersion tensor are distinct and there exist three unique normalized eigenvectors. The transformation matrix  $\mathbf{U}$  has the form

$$\mathbf{U} = \begin{pmatrix} \frac{v_1}{v} & -\frac{v_1 v_3}{v \sqrt{v_1^2 + v_2^2}} & -\frac{v_2}{\sqrt{v_1^2 + v_2^2}} \\ \frac{v_2}{v} & -\frac{v_2 v_3}{v \sqrt{v_1^2 + v_2^2}} & \frac{v_1}{\sqrt{v_1^2 + v_2^2}} \\ \frac{v_3}{v} & \frac{1}{v} \sqrt{v_1^2 + v_2^2} & 0 \end{pmatrix}. \quad (62)$$

The columns of  $\mathbf{U}$  form an orthonormal set of eigenvectors of  $\mathbf{D}$ . This transformation, however, becomes singular if  $v_1 = v_2 = 0$ . In this case, the dispersion tensor is diagonal and the transformation matrix  $\mathbf{U}$  is not needed.

[40] The dispersion tensor for an axisymmetric medium reduces to the isotropic case for equal transverse horizontal and vertical dispersivities. Since the eigenvectors are independent of the dispersivity coefficients and depend only on the flow velocity, the eigenvectors for the axisymmetric case must also be eigenvectors for the isotropic case. However, the converse is not true.

[41] For the generalized dispersion tensor the matrix  $\mathbf{Q}$  is given by

$$\mathbf{Q} = \begin{pmatrix} \sqrt{\alpha_L v + D_0} & 0 & 0 \\ 0 & \sqrt{\alpha_T v + D_0} & 0 \\ 0 & 0 & \sqrt{\alpha_T^H v + D_0} \end{pmatrix}, \quad (63)$$

including molecular diffusion. The displacement matrix  $\mathbf{B}$  has the form

$$\mathbf{B} = \begin{pmatrix} \frac{v_1}{v} \sqrt{2(\alpha_L v + D_0)} & -\frac{v_1 v_3 \sqrt{2(\alpha_T v + D_0)}}{v \sqrt{v_1^2 + v_2^2}} & -\frac{v_2 \sqrt{2(\alpha_T^H v + D_0)}}{\sqrt{v_1^2 + v_2^2}} \\ \frac{v_2}{v} \sqrt{2(\alpha_L v + D_0)} & -\frac{v_2 v_3 \sqrt{2(\alpha_T v + D_0)}}{v \sqrt{v_1^2 + v_2^2}} & \frac{v_1 \sqrt{2(\alpha_T^H v + D_0)}}{\sqrt{v_1^2 + v_2^2}} \\ \frac{v_3}{v} \sqrt{2(\alpha_L v + D_0)} & \sqrt{2 \frac{v_1^2 + v_2^2}{v^2} (\alpha_T v + D_0)} & 0 \end{pmatrix}. \quad (64)$$

[42] For the BF-dispersion tensor,  $\mathbf{Q}_{\text{BF}}$  is given by

$$\mathbf{Q}_{\text{BF}} = \begin{pmatrix} \sqrt{\alpha_L v + D_0} & 0 & 0 \\ 0 & \sqrt{\alpha_T^V v + D_0} & 0 \\ 0 & 0 & \sqrt{\alpha_T^H \frac{v_1^2 + v_2^2}{v} + \alpha_T^V \frac{v_3^2}{v} + D_0} \end{pmatrix}. \quad (65)$$

The displacement matrix  $\mathbf{B}_{\text{BF}}$  thus has the form

$$\mathbf{B}_{\text{BF}} = \begin{pmatrix} \frac{v_1}{v} \sqrt{2(\alpha_L v + D_0)} & -\frac{v_1 v_3 \sqrt{2(\alpha_T^H v + D_0)}}{v \sqrt{v_1^2 + v_2^2}} & -\frac{v_2}{\sqrt{v_1^2 + v_2^2}} \sqrt{2 \left[ \frac{\alpha_T^H (v_1^2 + v_2^2) + \alpha_T^V v_3^2}{v} + D_0 \right]} \\ \frac{v_2}{v} \sqrt{2(\alpha_L v + D_0)} & -\frac{v_2 v_3 \sqrt{2(\alpha_T^H v + D_0)}}{v \sqrt{v_1^2 + v_2^2}} & \frac{v_1}{\sqrt{v_1^2 + v_2^2}} \sqrt{2 \left[ \frac{\alpha_T^H (v_1^2 + v_2^2) + \alpha_T^V v_3^2}{v} + D_0 \right]} \\ \frac{v_3}{v} \sqrt{2(\alpha_L v + D_0)} & \sqrt{\frac{v_1^2 + v_2^2}{v^2}} (\alpha_T^V v + D_0) & 0 \end{pmatrix}. \quad (66)$$

#### 4. Numerical Simulations

[43] In this section several examples are presented to illustrate the particle tracking approach with axisymmetric dispersion. The BF-dispersion tensor is compared with the new form for a problem involving both vertical and horizontal flow in an axisymmetric medium. Calculations were carried out using the computer code FEHM [Zyvoloski *et al.*, 1997].

##### 4.1. Numerical Implementation

[44] To implement any particle-tracking algorithm, a method is needed for computing the velocity vector at all locations in the model domain in order to compute the deterministic portion of the particle transport vector, given by  $\mathbf{A}$  in equation (57). Although analytical solutions are possible for certain idealized situations, in general a finite difference or finite element model is the computational framework on which particle tracking methods are based. In the present study, the Finite Element Heat and Mass (FEHM) code is used to implement the random walk particle tracking methods derived above. FEHM is a control-volume, finite element model for simulating single-phase or two-phase flow through porous media in two or three dimensions. At present, this particle tracking method is restricted to structured grids, for which each control volume cell is brick shaped. To compute the velocity vector inside each cell, the velocity interpolation scheme of Pollock [1988] is used. With this method, velocity streamlines within a cell are computed using linear interpolation of the velocities at each face of the cell, as determined from the fluid flow solution. Particle trajectories are computed using equation (65), implemented by alternately computing the deterministic component  $\mathbf{A}\Delta t$ , followed by the random-walk component  $\sqrt{\Delta t}BZ$ . Particles crossing a cell boundary during the deterministic step are placed at the face of the adjacent cell at that same location. For particles that leave the cell during the random walk step, a simple search algorithm valid for structured grids is applied to determine the new cell and the local coordinates of the particles. Particles attempting to leave the model domain via the random-walk step are reflected back into the domain. The term  $\nabla \cdot \mathbf{D}$  in equation (8) is computed at the resolution of the finite element grid

using a simple finite difference scheme, as suggested by Tompson and Gelhar [1990]. The numerical model presented here is appropriate for dispersion tensors that vary relatively smoothly in space. The case of discontinuous changes in the dispersion tensor, such as resulting from large abrupt changes in porosity, are ongoing research issues [LaBolle *et al.*, 1996]. There are a variety of options for introducing particles into the system, recording the simulation results, and applying solute transport submodels to account for sorption and diffusion into stagnant pore water, such as in the matrix of a fracture-dominated porous medium. For details of these features, see Robinson [2000].

##### 4.2. Case I: Axisymmetric Dispersivity With Principal Axes Oblique to Flow Direction

[45] First, the case in which the principal axes of the dispersion tensor are aligned oblique to the flow direction is considered. A 3-dimensional grid with 10 nodes each in the  $x$ ,  $y$ , and  $z$  directions is used. The nodes are equally spaced in each direction with a spacing of 10 m. A porosity of 10% and permeability of  $10^{-14} \text{ m}^2$  is used in the simulation. The flow velocity is taken along the  $x$  axis with a value of  $-8.22 \times 10^{-11} \text{ m/s}$ . The dispersivity coefficients are chosen to be  $\alpha_1 = 2 \text{ m}$ ,  $\alpha_2 = 20 \text{ m}$ ,  $\alpha_3 = 12 \text{ m}$ , and  $\alpha_4 = -4 \text{ m}$ . [Note that the sign of  $\alpha_4$  is opposite to that of  $\alpha_3$  for  $\cos \theta > 0$  according to equation (17)]. The symmetry axis is taken to coincide with the line with direction cosines  $= (0.5, 0.866, 0)$ . A swarm of 10,000 particles is started at one end of the model domain, and allowed to flow and disperse toward the other end of the domain. The result after an elapsed time of  $6.95 \times 10^8$  days is shown in Figure 2. Note that the axes of the ellipsoid are lined up neither with the flow velocity, nor with the coordinate axes. The numerical results for the second moments of the plume are in good agreement with the theoretical values as listed in Table 1 and Table 2 for case I. The cosine of the angle between the major axis and the velocity vector is found from equation (16) to be 0.937, which is in good agreement with the numerical value calculated to be 0.928.

##### 4.3. Cases II and III: Comparison of New and BF Dispersion Tensors

[46] The Burnett and Frind and new form of the dispersion tensor are compared for a flow field similar to the previous case. The BF-tensor is applied with longitudinal dispersivity  $\alpha_L = 3 \text{ m}$ , transverse horizontal dispersivity  $\alpha_T^H = 1 \text{ m}$ , and transverse vertical dispersivity  $\alpha_T^V = 0.1 \text{ m}$ . In the BF-tensor, the axis of symmetry for the medium is assumed to be oriented along the vertical. The velocity is oriented at 45 degrees to the vertical. A swarm of 10,000 particles is allowed to flow and disperse. Results after elapsed times of  $2.32 \times 10^8$  and  $6.94 \times 10^8$  days are shown in Figure 3. The second moment of the plume is compared with the theoretical value in Table 2, case II ( $\lambda \cdot v = 1/\sqrt{2}$ ). Good agreement is obtained.

[47] The new form of the dispersion tensor, with coefficients given by equations (40a) and (40b), is used with the same flow field as described above with longitudinal horizontal dispersivity  $\alpha_L^H = 3 \text{ m}$ , longitudinal vertical dispersivity  $\alpha_L^V = 0.1 \text{ m}$ , transverse horizontal dispersivity  $\alpha_T^H = 0.1 \text{ m}$ , and transverse vertical dispersivity  $\alpha_T^V = 0.01 \text{ m}$ . When the flow velocity is normal to the axis of symmetry, i.e. flow is in the horizontal plane, the new form becomes identical to the

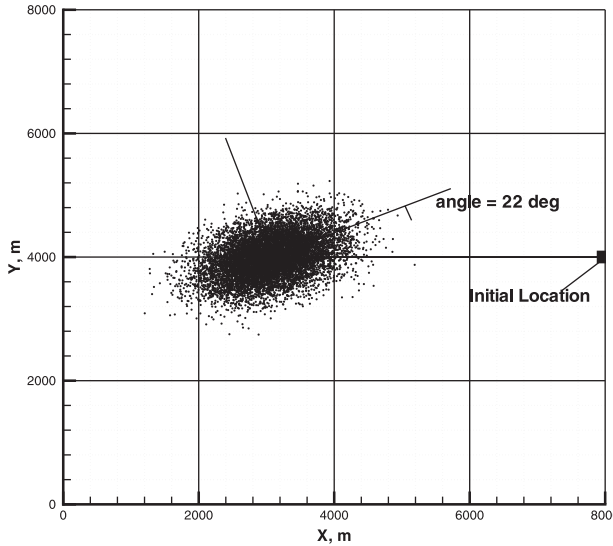


**Figure 2.** Axisymmetric dispersion tensor with principal axes at a angle  $\Phi$  to the direction of flow (case I).

BF-dispersion tensor. However, when the flow velocity is at an angle of 45 degrees, equations (41), (42), and (43) are used with the resulting values of  $\alpha_L = 1.55$  m,  $\alpha_T^H = 0.055$  m, and  $\alpha_T^V$  remains the same with a value of 0.01 m. This leads to a different shape for the dispersed particle cloud, shown for elapsed times of  $2.32 \times 10^8$  and  $6.94 \times 10^8$  days in Figure 4. The particle cloud is thicker in the direction perpendicular to the velocity in the  $x$ - $z$  plane compared to the BF-tensor, as would be expected comparing equations (53b) and (40b). The second moments for case III are compared in Table 2 with the theoretical result showing excellent agreement.

#### 4.4. 3-D Comparison of New and BF Dispersion Tensors

[48] In this example a transport problem similar to that discussed in *Burnett and Frind* [1987] is considered. The domain is 3-D, brick shaped, with  $x$ ,  $y$ , and  $z$  dimensions of 200 m, 15 m, and 200 m, respectively. The  $z$  axis is taken to point vertically upwards. Grid spacing in the  $x$  direction varies from 2.5 m to 5.62 m, that in the  $y$  direction is constant at 1 m, and that in the  $z$  direction varies from 7.3 m to 12.2 m.

**Table 1.** Description of Example Problems Used to Test and Compare Dispersion Models

Case	Description	Parameter Values
I	general, nonisotropic tensor $\lambda = (0.5, 0.866, 0)$ (Figure 2)	$t = 6.94 \times 10^8$ d $v_x = -8.22 \times 10^{-11}$ m/s, $v_y = v_z = 0$ m/s $\alpha_1 = 2$ m, $\alpha_2 = 20$ m, $\alpha_3 = 12$ m, $\alpha_4 = -4$ m
II	Burnett and Frind $\lambda \cdot v = 1/\sqrt{2}$ (Figure 3)	$t = 6.94 \times 10^8$ d $v_x = v_z = -8.22 \times 10^{-11}$ m/s, $v_y = 0$ m/s $\alpha_L = 3$ m, $\alpha_T^H = 1$ m, $\alpha_T^V = 0.1$ m
III	new form of tensor $\lambda \cdot v = 1/\sqrt{2}$ (Figure 4)	$t = 6.94 \times 10^8$ d $v_x = v_z = -8.22 \times 10^{-11}$ m/s, $v_y = 0$ m/s $\alpha_L^H = 3$ m, $\alpha_L^V = 1$ m, $\alpha_T^H = 1$ m, $\alpha_T^V = 0.1$ m

**Table 2.** Statistical Analysis of Plume Spreading Comparing Numerical and Analytical Values for the Square Root of Second Order Moments

Case	$\Delta x$ , m		$\Delta y$ , m		$\Delta z$ , m	
	Numerical	Theory	Numerical	Theory	Numerical	Theory
I	514	516	328	329	140	140
II	147	147	88	88	147	147
III	133	133	119	118	135	135

There are 50 nodes in the  $x$  direction, 16 in the  $y$  direction, and 22 in the  $z$  direction, with a total of 17600 nodes and 15435 elements. Permeability is taken to be uniform with a value of  $1.3 \times 10^{-12}$  m<sup>2</sup> and porosity is set to the value 0.35. Zero flux boundary conditions are imposed on the planes at  $x = 0$ ,  $y = 0$ ,  $y = 15$  m, and  $z = 0$ . On the  $z = 200$  m plane, a prescribed head is imposed: the head value is fixed in time but varies with the  $x$ -distance as a cosine function from  $h = 21$  m at  $x = 0$ , to  $h = 20$  m at  $x = 200$  m. The boundary on the  $x = 200$  m plane is kept at a constant head of  $h = 20$  m. The problem is first run to steady state, after which a tracer is introduced. This is done by releasing 10,000 particles in a small box dimensioned 10 m  $\times$  1 m  $\times$  1 m with center located at the position  $x = 10$  m,  $y = 7$  m,  $z = 180$  m. The particle swarm after 108,000 days is shown in Figures 5 and 6. Figure 5 shows the results for the Burnett and Frind tensor with  $\alpha_L = 10$  m,  $\alpha_T^H = \alpha_T^V = 1 \times 10^{-8}$  m. The results for the new form of the dispersion tensor with  $\alpha_L^H = 10$  m,  $\alpha_L^V = 0.1$  m, and  $\alpha_T^H = \alpha_T^V = 1 \times 10^{-8}$  m are shown in Figure 6. As expected, the BF-tensor predicts a significantly larger longitudinal dispersion. Thus it may be more appropriate to use the new form of the tensor in situations where the longitudinal vertical dispersivity is suspected to be different from the horizontal value.

#### 4.5. Example of the Influence of the $\nabla \cdot D$ Term on Particle Displacement

[49] As discussed in Section A.2, equation (57), the background drift term  $A$  contains the term  $\nabla \cdot D$  in addition

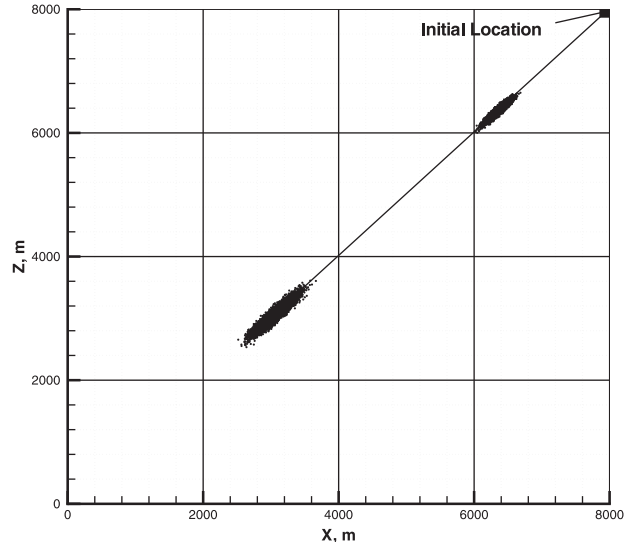


**Figure 3.** BF-dispersion tensor with flow at a  $45^\circ$  angle to the coordinate axes (case II).

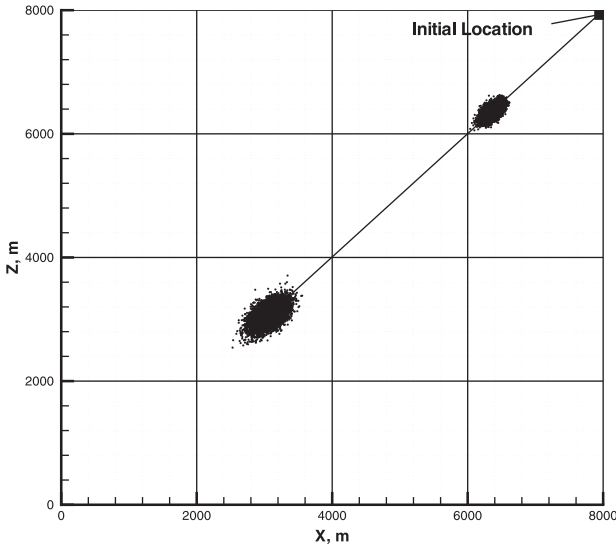


**Figure 4.** New form of dispersion tensor with flow at a  $45^\circ$  angle to the coordinate axes (case III).

to the usual fluid velocity. This term is often referred to as “spurious” or “noise-induced” drift [Risken, 1989]. The importance of this additional term is seen quite clearly in Figure 7, which shows the particle swarms calculated with and without the  $\nabla \cdot \mathbf{D}$  term for the model described in Section 4.4. In this example, the new form of the dispersion tensor is used, and for simplicity, the transverse dispersivities are set to a very low value,  $10^{-8}$  m. Horizontal longitudinal dispersivity is taken to be 10 m, and vertical longitudinal dispersivity 5 m. A swarm of 10,000 particles is started in a box  $0.1\text{ m} \times 0.1\text{ m} \times 0.1\text{ m}$  centered at the location of  $x = 10\text{ m}$ ,  $y = 7\text{ m}$  and  $z = 180\text{ m}$ , and the resulting particle locations after 108,000 days are shown in Figure 7. As seen in the figure, if the  $\nabla \cdot \mathbf{D}$  term is excluded from the computations, the particle cloud is displaced from the case with the  $\nabla \cdot \mathbf{D}$  term present. With the divergence term present, the particle cloud follows the streamline which passes through the starting point as indicated by the solid

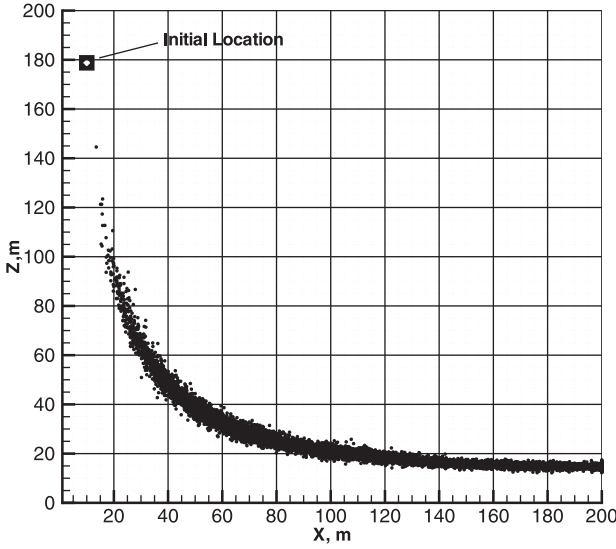


**Figure 5.** Example using BF-dispersion tensor in the absence of transverse dispersion.

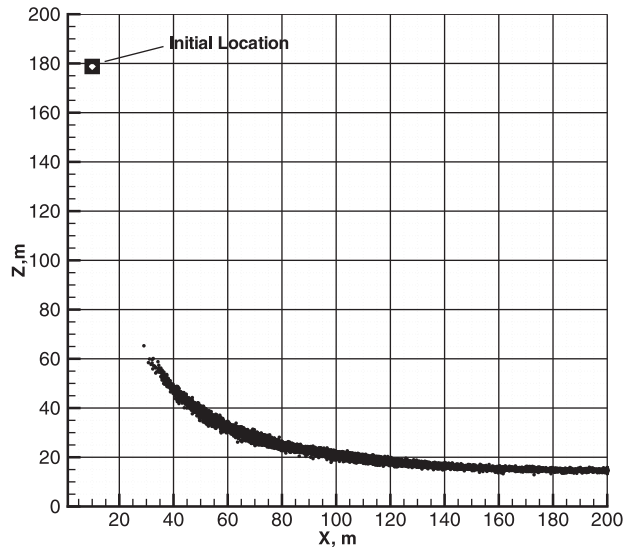


**Figure 6.** Example using the new form of the dispersion tensor in the absence of transverse dispersion.

curve. Thus it is essential to include this term when velocity gradients are present as has been pointed out previously [Kinzelbach and Uffink, 1991; LaBolle et al., 1996].

## 5. Discussion

[50] Although the dispersion tensor proposed by Burnett and Frind [1987] is a tensor by construction, it is limited to velocities that are close to perpendicular to the axis of symmetry. The new form of the dispersion tensor has four dispersivity coefficients:  $\alpha_L^V$  and  $\alpha_L^H$  for longitudinal dispersion, and  $\alpha_T^V$  and  $\alpha_T^H$  for transverse dispersion, in directions parallel and perpendicular, respectively, to the axis of symmetry. Although any direction may be chosen for the axis of

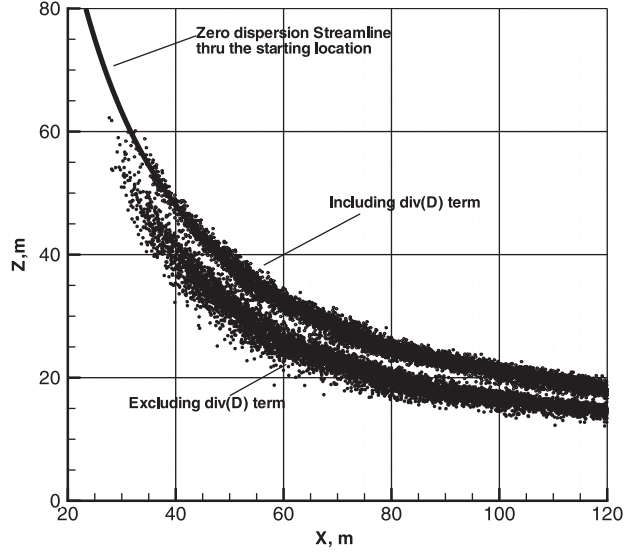


**Figure 7.** Comparison of particle tracking using the generalized form of the dispersion tensor for axisymmetric media with and without the  $\nabla \cdot \mathbf{D}$  term for the same problem as in section 4.4. The solid curve represent the streamline passing through the starting position of the particle cloud.

symmetry, the designations  $H$  and  $V$  are retained because in many practical applications a  $z$ -axis of symmetry is used to conform with previous theoretical studies and compilations of field data [e.g., *Gelhar*, 1997]. A distinction is made between horizontal and vertical longitudinal dispersivity  $\alpha_L^{H,V}$ , to account for anisotropic media with different longitudinal dispersion in the horizontal and vertical directions.

[51] In addition to the physical basis for proposing a new form of the dispersion tensor, the new form has an additional practical advantage in modeling dispersion in ground-water flow models for systems which exhibit large differences in horizontal and vertical longitudinal dispersivity. When developed using finite difference or finite element techniques, numerical groundwater flow models often employ grids with a much finer level of discretization in the  $z$  direction to capture heterogeneities of large lateral extent such as layered stratigraphy. Because in the *Burnett and Frind* [1987] formulation, the same longitudinal dispersivity applies in the vertical direction as is used for the horizontal directions, particles encountering a portion of the velocity field exhibiting a significant component of vertical flow will disperse in the  $z$  direction subject to a large longitudinal dispersivity that normally applies to the horizontal direction. As a consequence, particles will attempt to migrate via random walk several cells in the  $z$  direction unless very small time steps are used. Even when small time steps are taken, large dispersion and small grid spacing means that, on average, particles will disperse several cells during the course of advective transport through a single cell. Particle tracking methods designed to be accurate for advection-dominated transport with relatively small amounts of dispersion are not well suited to handle such highly diffusive situations. By contrast, the alternate form of the dispersion tensor proposed in the present study allows a small value of  $\alpha_L^V$  to be set, thereby limiting the amount of dispersion during vertical flow.

[52] Although little or no field data exists to determine the correct longitudinal dispersion in different directions of flow, it seems intuitive that in many situations, much smaller values of  $\alpha_L^H$  than  $\alpha_L^V$  would be appropriate. The new tensor developed here allows this situation to be modeled more efficiently using particle tracking methods. An avenue for potential future research is to construct detailed realizations of flow at different angles to the symmetry axis through model-generated heterogeneous media and to compare the results to equivalent homogeneous model simulations using the tensor proposed here. In both cases, particle tracking could be used, but in the heterogeneous simulations, the dispersion would be governed only by the local velocity variations that are computed as a matter of course (with no random-walk component), whereas for the dispersion tensor runs, a homogeneous flow field with random-walk particle tracking would be used. In this manner, the validity of the proposed tensor for capturing the dispersive characteristics could be examined and computed dispersivity parameters could be correlated to statistical parameters describing the heterogeneity.

## 6. Conclusion

[53] Several different options for the formulation of the dispersion tensor were explored for axisymmetric porous

media. A form-invariant formulation derived by *Poreh* [1965] based on symmetry arguments was developed and applied to axisymmetric media. The general form of the dispersion tensor, equation (3), is a symmetric, second order tensor that satisfies the necessary transformation rules upon changing from one coordinate system to another. It was shown that several well-known special cases follow from the general form after appropriate simplifications. For example, for the special case of an isotropic medium, with no preferred axis of symmetry, the tensor reduces to the commonly used form given in equation (23), and the individual terms of the tensor are shown to be functions of the fluid velocity  $v$ , and longitudinal and transverse dispersivities  $\alpha_L$ , and  $\alpha_T$ . For axisymmetric media a new form of the dispersion tensor was introduced with four dispersivity parameters: two longitudinal and two transverse dispersivities,  $\alpha_L^H$ ,  $\alpha_L^V$ , and  $\alpha_T^H$ ,  $\alpha_T^V$ , respectively, for flow parallel and perpendicular to the symmetry axis. The new tensor was contrasted with the dispersion tensor proposed by *Burnett and Frind* [1987] for describing dispersion in axisymmetric porous media.

[54] A series of test cases and example problems were presented to illustrate the method. Several of the tests focused on demonstrating the correct numerical implementation of the particle tracking method for the different forms of the dispersion tensor. All test cases yielded good agreement with theoretically based estimates of particle spreading. This included cases in which flow was not aligned with any of the coordinate axes, a critical test for any numerical transport model. A test case patterned after an example problem developed by *Burnett and Frind* [1987] exhibited behavior very similar to the results published in that paper. The alternate form of the tensor developed in the present study was shown to produce intuitively reasonable behavior when the longitudinal dispersion in the vertical direction was reduced to a low value. The example illustrated that particle tracking on grids with large aspect ratios (small  $z$  discretization compared to  $x$  and  $y$ ) should be more tractable using the new form of the dispersion tensor. Moreover, for axisymmetric media with large anisotropy, large spreading in the vertical direction due to use of the incorrect longitudinal dispersivity coefficient, an unavoidable trait in regions of vertical flow with the *Burnett and Frind* [1987] tensor, was shown to be reduced with the new tensor.

[55] The particle tracking algorithm discussed in the present study was implemented in the finite element computer code FEHM. The particular particle tracking algorithm developed is suitable for structured grids, that is, those in which computational control volumes are brick shaped. Current work is being performed to extend the algorithm to unstructured grids. This extension will require more general velocity interpolation schemes and particle search algorithms, but when completed, will allow the method to be employed for more complex geometries typically simulated using unstructured grids. That work will be reported on at a later date.

[56] The topic of the appropriateness of various forms of the dispersion tensor is the subject of ongoing theoretical and experimental studies. The present study illustrated straightforward methods for deriving the form of the tensor and the accompanying particle tracking displacement matrix  $B$  for axisymmetric media. Comparison with field observa-

tions or numerical experiments are needed to determine the functional form of the dispersion tensor for flow at an angle to the symmetry axis. Particle tracking methods were shown to provide an excellent computational framework to examine the different forms of the dispersion tensor. The theoretical methodology and particle tracking implementation should be transferable to new forms of the dispersion coefficient tensor in future modeling studies.

## Appendix A: Particle Tracking

### A.1. Random Walk: Langevin Equation

[57] Particle tracking approaches to describing solute transport involve superimposing on an instantaneous velocity field  $\mathbf{v}(\mathbf{r}, t)$ , a random walk representing dispersion and molecular diffusion. The partial differential equation for the solute concentration  $C$ , generally expressed by equation (1), is replaced by the Langevin equation written in differential form as

$$d\mathbf{r} = \mathbf{A}(\mathbf{r}, t)dt + \mathbf{B}(\mathbf{r}, t)dW(t), \quad (\text{A1})$$

for position vector  $\mathbf{r}(t)$ . The matrix  $\mathbf{A}$  represents the deterministic background drift determined by the fluid flow velocity  $\mathbf{v}$  and, in addition, contains contributions from the dispersion tensor as given in equation (57), and the matrix  $\mathbf{B}$  represents the direction and displacement distance for the random process  $dW$ . The differential  $dW(t)$  represents a Wiener process describing Brownian motion which incorporates effects of molecular diffusion and dispersion with the properties

$$\langle dW \rangle = 0, \quad (\text{A2})$$

and

$$\langle dW(t)dW(t) \rangle = dt\mathbf{I}, \quad (\text{A3})$$

where the angular brackets  $\langle \dots \rangle$  represent the ensemble mean, and  $\mathbf{I}$  denotes the unit matrix.

[58] The explicit finite difference form of the Langevin equation, equation (A1), using the Ito interpretation [Gardiner, 1997], can be expressed in matrix notation as

$$\mathbf{X}_n = \mathbf{X}_{n-1} + \mathbf{A}_{n-1}\Delta t_n + \mathbf{B}_{n-1}\mathbf{Z}_n\sqrt{\Delta t_n}, \quad (\text{A4})$$

with

$$dW_n = \mathbf{Z}_n\sqrt{\Delta t_n}, \quad (\text{A5})$$

for a time step  $\Delta t_n$ , where  $\mathbf{Z}_n$  represents a random vector and  $\mathbf{X}_n$  denotes the displacement vector after  $n$  steps.

### A.2. Fokker-Planck Equation

[59] To relate the displacement matrix  $\mathbf{B}$  appearing in the Langevin equation to the dispersion tensor  $\mathbf{D}$ , the Fokker-Planck equation, equivalent to the Langevin equation, equation (A1), for the conditional probability  $\mathcal{W}(\mathbf{r}, t|\mathbf{r}_0, t_0)$  of finding particles at  $(\mathbf{r}, t)$  given their initial position and time  $(\mathbf{r}_0, t_0)$ , is compared with the advection-diffusion-dispersion equation. The equivalent Fokker-Planck equation

is given by [Gardiner, 1997, p. 97; Jazwinski, 1970; Risken, 1989; Van Kampen, 1992]

$$\frac{\partial \mathcal{W}}{\partial t} = -\nabla \cdot \left[ \mathbf{A}(\mathbf{r}, t)\mathcal{W} \right] + \nabla : \nabla \left[ \frac{1}{2} \mathbf{B}\tilde{\mathbf{B}}\mathcal{W} \right], \quad (\text{A6})$$

where  $\tilde{\mathbf{B}}$  represents the transpose of matrix  $\mathbf{B}$ . In order to make the comparison, the Fokker-Planck equation must first be expressed in the form of the advection-diffusion-dispersion equation in which the divergence of the dispersive/diffusive flux appears. This may be achieved by writing the Fokker-Planck equation in the form

$$\frac{\partial \mathcal{W}}{\partial t} = -\nabla \cdot \left[ \left( \mathbf{A}(\mathbf{r}, t) - \frac{1}{2} \nabla \cdot \mathbf{B}\tilde{\mathbf{B}} \right) \mathcal{W} \right] + \nabla \cdot \left[ \frac{1}{2} \mathbf{B}\tilde{\mathbf{B}}\nabla \mathcal{W} \right]. \quad (\text{A7})$$

Comparing this modified form of the Fokker-Planck equation with the continuum-based advection-diffusion-dispersion equation given in equation (1) yields the identification

$$\mathcal{W}(\mathbf{r}, t|\mathbf{r}_0, t_0) = \frac{N_A}{N} \phi C(\mathbf{r}, t), \quad (\text{A8})$$

where  $N$  represents the number of particles and  $N_A$  denotes Avogadro's number. The matrix  $\mathbf{B}$  is related to the dispersion tensor  $\mathbf{D}$  by the identification

$$\frac{1}{2} \mathbf{B}\tilde{\mathbf{B}} = D, \quad (\text{A9})$$

and the displacement vector  $\mathbf{A}$  is related to the Darcy flux by

$$\mathbf{A} = \mathbf{v} + \frac{1}{\phi} \nabla \cdot \phi \mathbf{D}. \quad (\text{A10})$$

[60] One should expect that the mean and standard deviation derived for a single realization should be the same as that derived from an ensemble average. Indeed this is the case. The rate of change with time for the mean plume displacement as predicted by the advection-diffusion-dispersion equation for a single realization described by the concentration field  $C(\mathbf{r}, t)$  satisfies

$$\frac{d\bar{\mathbf{r}}}{dt} = \bar{\mathbf{A}}, \quad (\text{A11})$$

where for an arbitrary function  $f(\mathbf{r})$ , its mean is defined by

$$\overline{f(\mathbf{r})} = \int f(\mathbf{r})\phi C(\mathbf{r}, t)dV. \quad (\text{A12})$$

The rate of change of the second moment has the form

$$\begin{aligned} \frac{d}{dt} \overline{(\mathbf{r} - \bar{\mathbf{r}}) : (\mathbf{r} - \bar{\mathbf{r}})} &= 2\bar{\mathbf{D}} + \overline{(\mathbf{r} - \bar{\mathbf{r}}) : (\mathbf{A} - \bar{\mathbf{A}})} \\ &\quad + \overline{(\mathbf{A} - \bar{\mathbf{A}}) : (\mathbf{r} - \bar{\mathbf{r}})}, \end{aligned} \quad (\text{A13})$$

where the colon refers to the dyad or outer product for multiplying two tensors: thus  $(\mathbf{x} : \mathbf{y})_{ij} = x_{ij}y_j$ . Noteworthy is

the effect a spatially variable dispersion tensor, resulting from spatially variable flow velocity and porosity, has on the mean position of a contaminant plume.

[61] The results for the mean and standard deviation for a single realization may be compared with the results predicted by particle tracking using the Langevin equation and evaluating the ensemble average. Taking the ensemble average of equation (A4) yields

$$\frac{d\langle \mathbf{X} \rangle}{dt} = \lim_{\Delta t_n \rightarrow 0} \frac{\langle \mathbf{X}_n - \mathbf{X}_{n-1} \rangle}{\Delta t_n} = \langle \mathbf{A} \rangle, \quad (\text{A14})$$

in agreement with equation (A11). Likewise for the square of the standard deviation of the ensemble one obtains

$$\begin{aligned} \sigma_n^2 &= \langle (\mathbf{X}_n - \langle \mathbf{X}_n \rangle) : (\mathbf{X}_n - \langle \mathbf{X}_n \rangle) \rangle, \\ &= \sigma_{n-1}^2 + \langle \mathbf{B}_{n-1} \tilde{\mathbf{B}}_{n-1} \rangle \Delta t_n + (\langle (\mathbf{X}_{n-1} - \langle \mathbf{X}_{n-1} \rangle) : (\mathbf{A}_{n-1} - \langle \mathbf{A}_{n-1} \rangle) \rangle + \langle (\mathbf{A}_{n-1} - \langle \mathbf{A}_{n-1} \rangle) : (\mathbf{X}_{n-1} - \langle \mathbf{X}_{n-1} \rangle) \rangle) \Delta t_n \\ &\quad + \langle (\mathbf{A}_{n-1} - \langle \mathbf{A}_{n-1} \rangle) : (\mathbf{A}_{n-1} - \langle \mathbf{A}_{n-1} \rangle) \rangle \Delta t_n^2, \end{aligned} \quad (\text{A15})$$

in which terms linear in  $\mathbf{Z}_n$  vanish. Taking the limit as  $\Delta t_n \rightarrow 0$ , the time derivative of the squared standard deviation is given by

$$\begin{aligned} \frac{d\sigma^2}{dt} &= \langle \mathbf{B} \tilde{\mathbf{B}} \rangle + \langle (\mathbf{X} - \langle \mathbf{X} \rangle) : (\mathbf{A} - \langle \mathbf{A} \rangle) \rangle \\ &\quad + \langle (\mathbf{A} - \langle \mathbf{A} \rangle) : (\mathbf{X} - \langle \mathbf{X} \rangle) \rangle. \end{aligned} \quad (\text{A16})$$

This result is in agreement with equation (A13) provided equations (A9) and (A10) hold relating the displacement matrix to the dispersion tensor and drift term to the flow velocity. Thus the same functional form for the rate of change of the mean and standard deviation (and higher moments as well as can be easily demonstrated) are obtained for a single realization and for the ensemble mean. The values of the moments are expected to be equal in the limit of an infinite number of particles.

### A.3. Displacement Matrix $\mathbf{B}$

[62] To obtain the displacement matrix  $\mathbf{B}$  from the dispersion tensor  $\mathbf{D}$ , a transformation is carried out which diagonalizes the dispersion tensor [Risken, 1989, p. 57; Tompson et al., 1987]. The eigenvalue problem for  $\mathbf{D}$  reads

$$\mathbf{D} \zeta_\sigma = \sigma \zeta_\sigma, \quad (\text{A17})$$

with eigenvalue  $\sigma$  and eigenvector  $\zeta_\sigma$ . Because the dispersion tensor is symmetric, there exists an orthogonal transformation  $\mathbf{U}$  which diagonalizes  $\mathbf{D}$

$$\tilde{\mathbf{U}} \mathbf{D} \mathbf{U} = \hat{\mathbf{D}}, \quad (\text{A18})$$

where  $\hat{\mathbf{D}}$  is a diagonal matrix with diagonal elements  $\sigma_i$ , and  $\mathbf{U}$  satisfies the relations

$$\mathbf{U} \tilde{\mathbf{U}} = \tilde{\mathbf{U}} \mathbf{U} = \mathbf{I}. \quad (\text{A19})$$

Expressing  $\hat{\mathbf{D}}$  in the form

$$\hat{\mathbf{D}} = \mathbf{Q} \tilde{\mathbf{Q}}, \quad (\text{A20})$$

with  $\mathbf{Q}$  diagonal ( $\tilde{\mathbf{Q}} = \mathbf{Q}$ ), then gives

$$2D = 2\mathbf{U} \hat{\mathbf{D}} \tilde{\mathbf{U}} = 2\mathbf{U} \mathbf{Q} \tilde{\mathbf{Q}} \tilde{\mathbf{U}} = 2\mathbf{U} \mathbf{Q} \tilde{\mathbf{U}} \mathbf{Q} = \mathbf{B} \tilde{\mathbf{B}}. \quad (\text{A21})$$

From this relation it follows that the displacement matrix  $\mathbf{B}$  is given by [Tompson et al., 1987]

$$\mathbf{B} = \sqrt{2} \mathbf{U} \mathbf{Q}, \quad (\text{A22})$$

with the matrix  $\mathbf{Q}$  equal to the square root of the eigenvalues of  $\mathbf{D}$

$$\mathbf{Q} = \begin{pmatrix} \sqrt{\sigma_1} & 0 & 0 \\ 0 & \sqrt{\sigma_2} & 0 \\ 0 & 0 & \sqrt{\sigma_3} \end{pmatrix}. \quad (\text{A23})$$

### Appendix B: Nonuniqueness of Displacement Matrix $\mathbf{B}$

[63] The displacement matrix  $\mathbf{B}$  is not unique. In certain cases this nonuniqueness can be exploited to advantage in the numerical implementation of the random walk process [Tompson et al., 1987]. Because only the product  $\mathbf{B} \tilde{\mathbf{B}}$  is determined by the dispersion tensor  $\mathbf{D}$ , it is possible to multiply  $\mathbf{B}$  by an orthogonal matrix on the right and preserve equation (A21) [Gardiner, 1997, p. 97]. Thus if  $\mathbf{B}' = \mathbf{B} \mathbf{S}$  with  $\mathbf{S}$  an orthogonal matrix, then  $\mathbf{B}' \tilde{\mathbf{B}}' = \mathbf{B} \tilde{\mathbf{B}}$ .

[64] The orthogonal transformation  $\mathbf{U}$  itself may not be unique leading to a nonunique displacement matrix  $\mathbf{B}$ . For example, for an isotropic medium, the dispersion tensor has two degenerate eigenvalues, and hence there exists an infinity of different transformations  $\mathbf{U}$  which diagonalize  $\mathbf{D}$ . To determine how the nonuniqueness of  $\mathbf{U}$  affects the Langevin equation and hence a random walk path, note that if there exist two such transformations,  $\mathbf{U}$  and  $\mathbf{U}'$ , which diagonalize  $\mathbf{D}$ , then it follows that

$$\tilde{\mathbf{U}}' \mathbf{D} \mathbf{U}' = \tilde{\mathbf{U}} \mathbf{D} \mathbf{U} = \hat{\mathbf{D}}, \quad (\text{B1})$$

or

$$\begin{aligned} \mathbf{D} &= (\tilde{\mathbf{U}}' \tilde{\mathbf{U}}) \mathbf{D} (\mathbf{U}' \tilde{\mathbf{U}}), \\ &= \tilde{\mathbf{S}} \mathbf{D} \mathbf{S}, \end{aligned} \quad (\text{B2})$$

with  $\mathbf{S}$  defined as

$$\mathbf{S} = \mathbf{U}' \tilde{\mathbf{U}}. \quad (\text{B3})$$

The matrix  $\mathbf{S}$  is orthogonal since  $\mathbf{U}$  and  $\mathbf{U}'$  are orthogonal. It follows from equation (B-2) that  $\mathbf{S}$  and  $\mathbf{D}$  commute

$$[\mathbf{S}, \mathbf{D}] = \mathbf{S} \mathbf{D} - \mathbf{D} \mathbf{S} = 0. \quad (\text{B4})$$

It likewise follows that  $\mathbf{S}$  and  $\mathbf{B}$  commute. Substituting  $\tilde{\mathbf{B}}\tilde{\mathbf{B}}$  for  $\mathbf{D}$  in equation (B-2) yields

$$\tilde{\mathbf{B}}\tilde{\mathbf{B}} = \tilde{\mathbf{S}}\tilde{\mathbf{B}}\tilde{\mathbf{B}}\mathbf{S} = \tilde{\mathbf{S}}\mathbf{B}\tilde{\mathbf{S}}\tilde{\mathbf{B}}\mathbf{S} = (\tilde{\mathbf{S}}\mathbf{B}\mathbf{S}) (\tilde{\mathbf{S}}\mathbf{B}\mathbf{S}). \quad (\text{B5})$$

Therefore  $\mathbf{B} = \tilde{\mathbf{S}}\mathbf{B}\mathbf{S}$  or  $[\mathbf{S}, \mathbf{B}] = 0$ . Denoting the displacement matrix corresponding to  $\mathbf{U}'$  by  $\mathbf{B}'$ , it follows that

$$\mathbf{B}' = \mathbf{S}\mathbf{B}. \quad (\text{B6})$$

Thus

$$\begin{aligned} d\mathbf{r}' &= \mathbf{A}dt + \mathbf{S}\mathbf{d}W, \\ &= \mathbf{A}dt + \mathbf{B}\mathbf{S}\mathbf{d}W, \\ &= \mathbf{A}dt + \mathbf{B}\mathbf{d}W, \end{aligned} \quad (\text{B7})$$

where the latter equality follows because  $\mathbf{S}\mathbf{d}W(t)$  is also a Wiener process, since  $\mathbf{S}$  is orthogonal [Gardiner, 1997, p. 98], and therefore statistically  $\mathbf{S}\mathbf{d}W = \mathbf{d}W$ . It follows that

$$d\mathbf{r}' = d\mathbf{r}. \quad (\text{B8})$$

Consequently,  $\mathbf{U}'$  and  $\mathbf{U}$  lead to statistically indistinguishable random walks.

[65] **Acknowledgments.** The authors thank Daniel Tartakovsky at LANL for helpful discussions and two anonymous reviews whose comments greatly improved the manuscript. This work was supported by the Yucca Mountain Site Characterization Program Office as part of the Civilian Radioactive Waste Management Program. This project is managed by the U. S. Department of Energy, Yucca Mountain Site Characterization Project.

## References

- Ahlstrom, W. W., H. P. Foote, P. C. Arnett, C. R. Cole and R. J. Serne, Multicomponent mass transport model: Theory and numerical implementation (discrete parcel random walk version), *Rep. BNWL 2127*, Battelle Northwest Lab., Richland, Wash., 1977.
- Anderson, M. P., Using models to simulate the movement of contaminants through groundwater flow systems, *CRC Crit. Rev. Environ. Control*, 9, 97–156, 1979.
- Batchelor, G. K., *The Theory of Homogeneous Turbulence*, Cambridge Univ. Press, 1959.
- Bear, J., *Dynamics of Fluids in Porous Media*, 764 pp., Dover, Mineola, N. Y., 1972.
- Burnett, R. D., and E. O. Frind, Simulation of contaminant transport in three dimensions, 2, Dimensionality effects, *Water Resour. Res.*, 23, 695–705, 1987.
- Cirpka, O. A., E. O. Frind, and R. Helmig, Numerical methods for reactive transport on rectangular and streamline-oriented grids, *Adv. Water Res.*, 22, 711–728, 1999.
- Dagan, G., *Flow and Transport in Porous Formations*, 465 pp., Springer-Verlag, New York, 1984.
- de Marsily, G., *Quantitative hydrology*, 440 pp., Academic, San Diego, Calif., 1986.
- Fabriol, R., J.-P. Sauty, and G. Ouzounian, Coupling geochemistry with a particle tracking transport model, *J. Contam. Hydrol.*, 13, 117–129, 1993.
- Gardiner, C. W., *Handbook of Stochastic Methods*, 2nd ed., 442 pp., Springer-Verlag, New York, 1997.
- Gelhar, L. W., Perspectives on field-scale application of stochastic subsurface hydrology, in *Subsurface Flow and Transport: A Stochastic Approach*, edited by G. Dagan and S. P. Neuman, pp. 157–176, Cambridge Univ. Press, New York, 1997.
- Gelhar, L. W., and C. L. Axness, Three-dimensional stochastic analysis of macrodispersion in aquifers, *Water Resour. Res.*, 19, 161–180, 1983.
- Jazwinski, A. H., *Stochastic Processes and Filtering Theory*, 376 pp., Academic, San Diego, Calif., 1970.
- Jensen, K. H., K. Bitsch, and P. L. Bjerg, Large-scale dispersion experiments in a sandy aquifer in Denmark: Observed tracer movements and numerical analyses, *Water Resour. Res.*, 29, 673–696, 1993.
- Kinzelbach, W., and G. Uffink, The random walk method and extensions in groundwater modeling, in *Transport Processes in Porous Media*, edited by J. Bear and M. Y. Corapcioglu, pp. 761–787, Kluwer Acad., Norwell, Mass., 1991.
- LaBolle, E. M., G. E. Fogg, and A. F. B. Thompson, Random-walk simulation of transport in heterogeneous porous media: Local mass-conservation problem and implementation methods, *Water Resour. Res.*, 32, 583–593, 1996.
- Morse, P. M., and H. Feshback, *Methods of Theoretical Physics*, part I, 997 pp., McGraw-Hill, New York, 1953.
- Neuman, S. P., Universal scaling of hydraulic conductivities and dispersivities in geologic media, *Water Resour. Res.*, 26, 1749–1758, 1990.
- Neuman, S. P., C. L. Winter, and C. M. Newman, Stochastic theory of field-scale Fickian dispersion in anisotropic porous media, *Water Resour. Res.*, 23, 453–466, 1987.
- Pollock, D. W., Semianalytical computation of path lines for finite-difference models, *Ground Water*, 26, 743–750, 1988.
- Poreh, M., The dispersivity tensor in isotropic and axisymmetric media, *J. Geophys. Res.*, 70, 3909–3914, 1965.
- Risken, H., *The Fokker-Planck Equation: Methods of Solution and Applications*, 2nd ed., 472 pp., Springer-Verlag, New York, 1989.
- Robertson, R. P., The invariant theory of isotropic turbulence, *Proc. Philos. Soc.*, 36, 209–223, 1940.
- Robinson, B. A., Saturated zone transport methodology and transport component integration, *Rep. MDL-NBS-HS-000010*, Civ. Radioactive Waste Manage. Syst. M&O, Las Vegas, Nev., 2000.
- Robson, S. G., Application of digital profile modeling techniques to groundwater solute transport at Barstow, California, *U.S. Geol. Surv. Water Supply Pap.*, 2050, 1978.
- Scheidegger, A. E., General theory of dispersion in porous media, *J. Geophys. Res.*, 66, 3273–3278, 1961.
- Tchelepi, H., F. Orr, N. Rakotomalala, S. Salin, and R. Woumeni, Dispersion, permeability, heterogeneity, and viscous fingering: Experimental simulations and particle-tracking simulations, *Phys. Fluids*, A5, 1558–1574, 1993.
- Tompson, A. F. B., Numerical simulation of chemical migration in physically and chemically heterogeneous porous media, *Water Resour. Res.*, 29, 3709–3726, 1993.
- Tompson, A. F. B., and D. E. Dougherty, On the use of particle tracking methods for solute transport in porous media, in *Computational Methods in Water Resources*, vol. 2, *Numerical Methods for Transport and Hydrologic Processes*, edited by M. Celia et al., pp. 227–232, Elsevier Sci., New York, 1988.
- Tompson, A. F. B., and L. W. Gelhar, Numerical simulation of solute transport in three-dimensional, randomly heterogeneous porous media, *Water Resour. Res.*, 26, 2541–2562, 1990.
- Tompson, A. F. B., E. G. Vomvoris, and L. W. Gelhar, Numerical simulation of solute transport in randomly heterogeneous porous media: Motivation, model development and application, *Rep. UCID 21287*, Lawrence Livermore Natl. Lab., Livermore, Calif., 1987.
- Tompson, A. F. B., A. L. Schafer, and R. W. Smith, Impacts of physical and chemical heterogeneity on cocontaminant transport in a sandy porous medium, *Water Resour. Res.*, 32, 801–818, 1996.
- Van Kampen, N. G., *Stochastic Processes in Physics and Chemistry*, 465 pp., North-Holland, New York, 1992.
- Zheng, C., and C. D. Bennett, *Applied Contaminant Transport Modeling: Theory and Practice*, 440 pp., Van Nostrand Reinhold, New York, 1995.
- Zyvoloski, G. A., B. A. Robinson, Z. V. Dash and L. L. Trease, User's manual for the FEHM Application—A Finite-Element Heat- and Mass-Transfer code, *Rep. LA-13306-M UC-800, UC-802*, Los Alamos Natl. Lab., Los Alamos, N. M., 1997.